Master's Degree Thesis
ISRN: BTH-AMT-EX--2005/D-11--SE

Load Calculation and Simulation of an Asphalt Roller

Amer Mohamed

Department of Mechanical Engineering
Blekinge Institute of Technology
Karlskrona, Sweden

2005

Supervisor: Kjell Ahlin, Professor Mech. Eng.

Load Calculation and Simulation of an Asphalt Roller

Amer Mohamed

Department of Mechanical Engineering

Blekinge Institute of Technology

Karlskrona, Sweden

2005

Thesis submitted for completion of Master of Science in Mechanical Engineering with emphasis on Structural Mechanics at the Department of Mechanical Engineering, Blekinge Institute of Technology, Karlskrona, Sweden.

Abstract:

Free body diagrams of an Asphalt Roller were designed for several load cases and used for an optimisation study. Assumptions for the load calculations for each load case were carried out in MATLAB®.

The roller was built in I-DEAS® and the results were compared with the theoretical results.

Keywords:

Asphalt Roller, Optimisation, Drums, Forks, Rigid body, Steering Hitch, Free body diagram, Roller model, Theoretical model, MATLAB, I-DEAS simulation, Verification.

Acknowledgements

This work was carried out at DYNAPAC Compaction Equipment AB, Karlskrona, Sweden, under the supervision of Tyra Lycken and Prof. Kjell Ahlin.

The work is a part of a research project, which is going on in DYNAPAC Compaction Equipment AB, Karlskrona, Sweden.

This thesis work was initiated in October 2004.

I wish to express my sincere appreciation to MSc. Tyra Lycken and Prof. Kjell Ahlin for their guidance and professional engagement throughout the work at DYNPAC AB. I wish to thank Tomas Rommer for valuable support and advice.

Karlskrona, March 2005

Amer Mohamed

Contents

1 Notation

MT	Total mass of the roller (kg)
MD1	Front drum mass (kg)
MVF	Front vibrated mass fork (kg)
MDF	Front drive fork mass (kg)
MS	Front mass section A-A (kg)
MK	Rear mass section B-B (kg)
MH	Rear mass section C-C (kg)
MVFB	Rear vibrated mass fork (kg)
MVF	Rear vibrated mass fork (kg)
MD_2	Rear drum mass (kg)
MTR	Trailer mass (kg)
G	Acceleration of gravity
J	Mass moment of inertia ($kg.m^2$)
R	Radius of the drums (m)
FB_1	External longitudinal braking force at the front drum (N)
FB_2	External normal force at the front drum (N)
FB_3	External longitudinal braking force at the rear drum (N)
FB_4	External normal force at the rear drum (N)
FYF	External lateral force of the front drum (N)
FYB	External lateral force of the rear drum (N)
FX	Internal forces in x-x direction (N)
FX	Internal forces in y-y direction (N)
FX	Internal forces in z-z direction (N)
M_{X-X}	Torque about x-x axis (Nm)

M_{Y-Y}	Torque about y-y axis (Nm)
M_{Z-Z}	Torque about z-z axis (Nm)
h_F	The coefficient of friction of the Front drum
h_R	The coefficient of friction of the Front drum
W_1	The width of the drums (m)
KX_1	Linear translation stiffness in x-x axis for the vibrated side (N/m)
KX_2	Linear translation stiffness in x-x axis for the drive side (N/m)
KY_1	Linear translation stiffness in y-y axis for the vibrated side (N/m)
KY_2	Linear translation stiffness in y-y axis for the drive side (N/m)
KZ_2	Linear translation stiffness in z-z axis for the vibrated side (N/m)
KZ_2	Linear translation stiffness in z-z axis for the drive side (N/m)
KCX_1	Torsion (rotational) stiffness in x-x axis for the vibrated (Nm/rad)
KCX_2	Torsion (rotational) stiffness in x-x axis for the drive side (Nm/rad)
KCZ_1	Torsion (rotational) stiffness in z-z axis for the vibrated (Nm/rad)
KCZ_2	Torsion (rotational) stiffness in z-z axis for the drive side (Nm/Rad)
q	The inclined surface angle (degree)
X	The displacement in x-x axis (m)
Y	The displacement in y-y axis (m)
Z	The displacement in z-z axis (m)
X_T	C.G of the total mass in x-direction (m)

X_1	C.G of the front drum mass in x-direction (m)
X_3	C.G of the rear drum mass in x-direction (m)
X_4	Distance between C.G of MF and MD_1
X_5	Distance between C.G of MR and MD_2
X_{VF}	C.G of the mass MVF to the steering hitch in x-direction (m)
X_{DF}	C.G of the mass MDF to the steering hitch (m) in x-direction
X_{VR}	C.G of the mass MVFB to the steering hitch (m) in x-direction
X_{DR}	C.G of the mass MDFB to the steering hitch in x-direction
X_{LOAD}	Internal load points 3,4,10 and 11 to the steering hitch (m)
X_{100}	The location of the front section A-A to the steering hitch in x-direction (m)
X_{300}	The location of the front section B-B to the steering hitch in x-direction (m)
X_{500}	The location of the front section C-C to the steering hitch in x-direction (m)
X_{LIFT1}	The location of the front eyelet to the steering hitch in x-direction (m)
X_{LIFT2}	The location of the rear eyelet to the steering hitch in x-direction (m)
X_{mH}	Distance to the mass MH for the section C.C (m)
X_{mk}	Distance to the mass MH for the section B.B (m)
X_{ms}	Distance to the mass MS for the section A.A (m)
X_A	Distance to the front body of the roller MF

X_B	Distance to the rear body of the roller MR
Y_{VF}	Distance to the front vibrated fork (m)
YDF	Distance to the front drive fork (m)
Y_{VB}	Distance to the rear vibrated fork (m)
Y_{DB}	Distance to the rear drive fork (m)
Y_{LOAD}	Distance to the internal loads3, 4, 10 and 11 (m)
Y_{100}	Distance of the vibrated rubber to the drums (m)
Y_{200}	Distance of the drive rubber to the drums (m)
Z_T	Distance to the total mass of the roller
Z_S	Distance to the centre of the drums from the steering hitch (m)
Z_{VF}	Distance to the front vibrated fork MVF (m)
Z_{DR}	Distance to the rear vibrated fork MVFB (m)
Z_{DF}	Distance to the front drive fork MDF (m)
Z_{VR}	Distance to the rear drive fork MDFB (m)
Z_{LOAD}	Distance to the internal loads 3,4,10 and 11 (m)
Z_3	Distance to the front mass MF (m)
Z_4	Distance to the rear mass MR (m)
Z_5	Distance to the pulling and towing eyelet (m)
Z_{100}	Distance to the C.G. of the mass MS (m)
Z_{200}	Distance to the C.G. of the mass MS (m)
Z_{10}	Distance to the load points of the front forks (m)

Z_{11}	Distance to the load points of the front forks (m)
j_x	Rotational angle about x-x axis
j_z	Rotational angle about z-z axis

2 Introduction

2.1 Description of an Asphalt Roller

Asphalt Roller shown in figure 2.1 is a Compacter having a drum (Roll or horizontal cylinder) used to compact soil, asphalt or other materials through the application of combined static and dynamic forces (weight and vibrations) to increase the load bearing – capacity of the surface. The machine may have one or more drums, which may or may not be powered for propulsion. The machine may have drive members such as rubber tires in addition to the drums. The Centrifugal force is normally produced by one or more rotating off-centre weights, which produces a cyclic movement of the drum. The drums and drive wheels may be smooth or may include projections designed for specific compaction purposes. These projections vary as to a material, size and shape.

Figure2.1 Asphalt Roller.

2.2 Background

During the last years the internal demands from the industries have been intensified to get higher performance from Asphalt Rollers and make improvements for the design. One specific demand is the calculation of the static, quasi-static and dynamic loads, which affect an Asphalt Roller. These perfect calculations aid in improving the Roller and eventually increasing the performance.

There are many types of Rollers for different purposes. Rollers for soil and asphalt compaction are the most general type. Soil and Asphalt compaction can be carried out with either static compaction with wheels of rubber or dynamic compaction with vibrating Rollers that have drums made of steel (when two vibrating drums are used the number of passes required decreases while the Roller capacity increases).

It is customary to classify compaction with respect to the frequency to the applied load:

- Static loading has zero frequency.
- Impact loading has a low frequency up to some tens of Hertz.
- Dynamic loading has high frequency.

For a static and vibrated Asphalt Roller the most important parameters that influence the compaction effort are:

- The static linear load (N/m): Defined as the weight of the drum divided by the drum width. If the linear static loads increase noticeably the pressure in the material increases.
- Drum diameter: large diameter reduces rolling resistance.
- The drum width: wider diameter results in a greater surface coverage per pass.
- Vibration amplitude.
- Frequency: Defined as the number of complete cycles of the vibrating mechanism per unit time.
- The speed.

In this work an Asphalt Roller of DYNAPAC Compaction Equipment AB was studied. The various parts of the Roller can be seen in figure 2.2. It is a self–propelled compaction machine that consists of two steel drums, which

can be static or vibratory to compress the Asphalt and the Soil where the drum vibration adds a dynamic load to the static Roller weight to create a greater total compactive effort as well as reduces the friction. Furthermore the Asphalt Roller consists of an Engine and its supports, Water tank, Oil tank, Driver seat, Forks, Steering Hitch, ROPs and Yoke. The forks join the drum and the frames. The Steering Hitch attaches the front body with the rear one to make the Asphalt Roller tandem. The ROPs (Roll over protection structure) protects the driver if the Roller turns upside down. Yoke contains the Pivot bearing with a hydraulic cylinder that makes the rear drum turn to the left and right. It is significant benefit if the Asphalt Roller can operate over a wide range of field conditions, for example, on different types of Asphalt and at high altitudes [1].

The main aims were specified below to study this type of Roller:

- The investigation of the theoretical model for different load cases.
- Building of a theoretical model in MATLAB®.
- Calculating the Static and Quasi-static loads for different load cases.
- Building an I-DEAS™ simulation model for comparison with theoretical model.

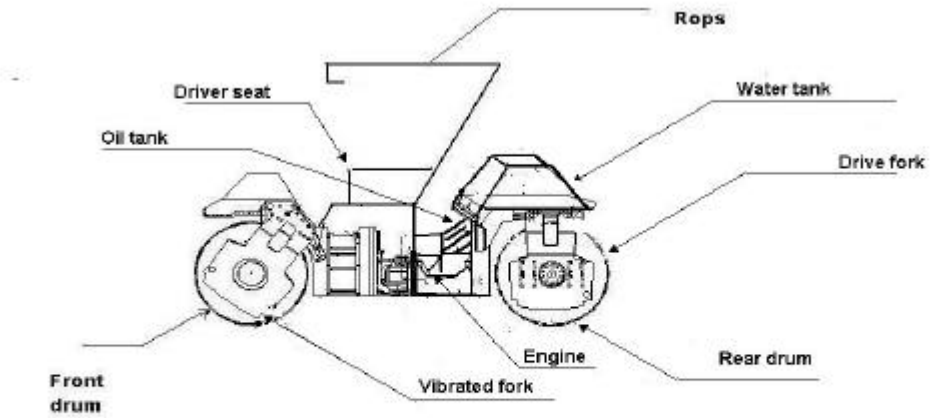

Figure2.2. Asphalt Roller parts.

The previous work in this field was included a study on this machine and calculating the dynamic forces at the engine, the drums and forks. This thesis work dealt with Static and Quasi-static loads for different load cases. A mathematical model was built. It was a set of equations that described the forces and its corresponding moments for several important parts which are specified as rigid bodies in 3-D. MATLAB® programme was designed for solving the system of equations. The programme is useful for the designers to get the knowledge about the Static and Quasi –static loads which should be considered during the design and use it for different types of Roller by varying the input data.

2.3 Assumptions and simplifications

- The Asphalt Roller was specified as a number of solid rigid bodies' which define as bodies whose changes in shape are negligible compared with the overall dimensions of the body and that means there is no deformation and no internal energy can be stored and the mass is constant.
- The internal load points 5, 8 and 9 of the main sections, which will mention later, were placed in z level of the gravity (the balance point) of the section masses to decrease the forces and moments calculations.
- The centre of the gravity of the masses, that is the point through which the force of gravity seems to act, was placed at y- axis in the model, except the forks in order to decrease the effect of the moment in x-axis and keep the Roller symmetric as possible.
- The longitudinal and normal external forces between the ground and the edges of the drums assumed equal to each other in each side in the theoretical model to avoid unnecessary complexity during the calculations.
- The inclination of the geometry of the rubber elements was changed to global system.

2.4 Project description

The method used to solve this type of investigations was the theoretical model in MATLAB® and the Mechanical system simulation performed in I-DEAS® for verifications and getting a deeper insight about the element forces, reactions, mode shapes and displacements owing to I-DEAS® ability to produce virtual prototypes. MATLAB-codes were written to carry on the calculations of the theoretical model and evaluate different loads that the Asphalt Roller is subjected during the work. General available I-DEAS model was used to build a basic simulation model of the Asphalt Roller for different load cases by getting the parameters:

- The masses.
- The location of the centre of gravities.
- Number and the Geometry of the rubber elements,
- Physical properties of the linear translation spring of the rubber elements.
- Important main section parts of the Asphalt Roller.

3 Theory

The load cases were studied:

- Gravity load case.
- Acceleration/Retardation load case.
- Lifting load case.
- Pulling load case.
- Maximum torque load case.
- Towing load case.
- Steering loads under gravity.
- Steering loads under gravity and lateral acceleration considerations.

The external and internal loads acting on the Asphalt Roller can be summed into one force vector having the following components:

- Longitudinal force (FX): the component of the force vector in x-axis with a positive value to the right.
- Side (lateral) force (FY): the component of the force vector in y-axis with a positive value through the paper.
- Normal force (FZ): the component of the force vector in z-axis with a positive value upward.

The external and internal moments acting on the Asphalt Roller can be summed into one moment vector having the following components:

- Moment (M_{X-X}): the component of the moment vector tending to rotate the roller about x-axis with a clockwise positive value.
- Moment (M_{Y-Y}): the component of the moment vector tending to rotate the roller about y-axis with a clockwise positive value.
- Moment (M_{Z-Z}): the component of the moment vector tending to rotate the roller about z-axis with a clockwise positive value.

The location of zero -centre was specified at the Steering Hitch.

3.1 External and Internal load points

The Asphalt Roller was assumed as eleven rigid bodies after making three main sections (A, B and C). The required forces and corresponding moments were calculated at several important load points; some of them were external and others internal as shown in figure 3.1. The locations of these points were scaled from the Steering Hitch which was considered as a reference point. The inclination surface angle q uphill was considered during the calculations.

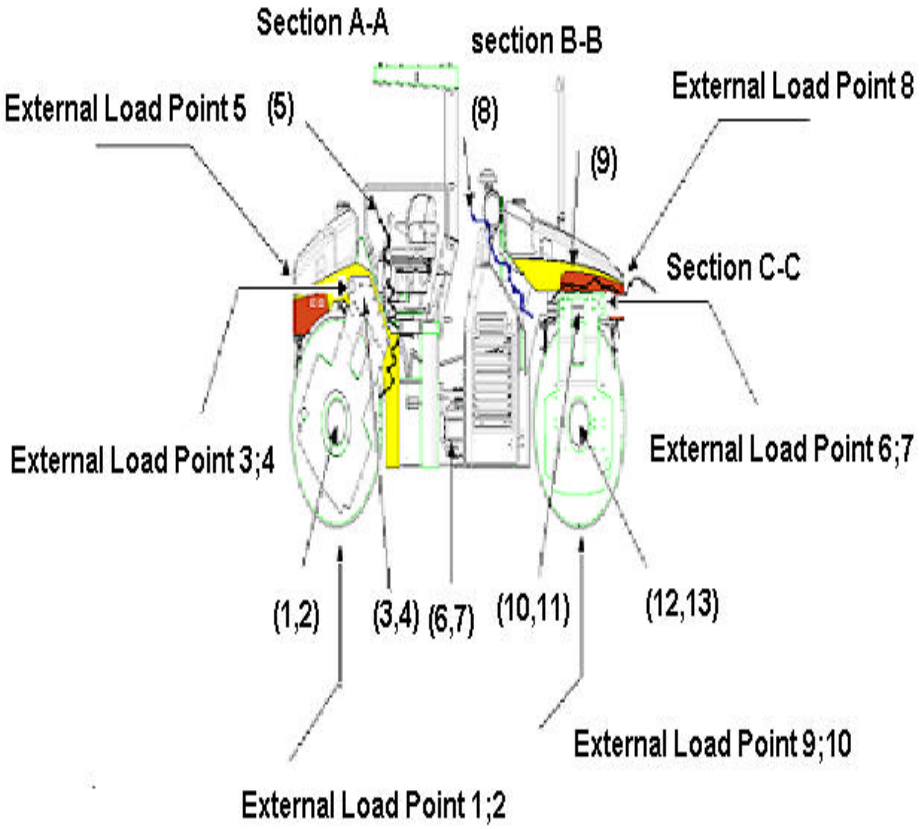

Figuer3.1. External and Internal load points.

3.2 Gravity load case

Gravity is one of the universal forces of nature. It is an attractive force between all things. The gravitational force between two objects is proportional to the product of their masses and inversely proportional to the square of the distance between them. According to Newton's first law the object at rest, tends to stay at rest and an object in motion tends to stay in motion with the same speed and in the same direction unless acted upon by an unbalanced force. The condition of static load deals with the description of the conditions of balanced force, which are both necessary and sufficient to maintain the state of equilibrium of any engineering structure so that to model this load case the Asphalt Roller should be kept in equilibrium conditions and that means the resultant forces (R_X, R_Y and R_Z) and corresponding resultant moments (MR_X, MR_Y and MR_Z) acting on it were zero [2]. Thus, the equilibrium equations:

$$R_X = \sum FX = 0 \tag{3.1}$$

$$R_Y = \sum FY = 0 \tag{3.2}$$

$$R_Z = \sum FZ = 0 \tag{3.3}$$

$$MR_X = \sum M_X = 0 \tag{3.4}$$

$$MR_Y = \sum M_Y = 0 \tag{3.5}$$

$$MR_Z = \sum M_Z = 0 \tag{3.6}$$

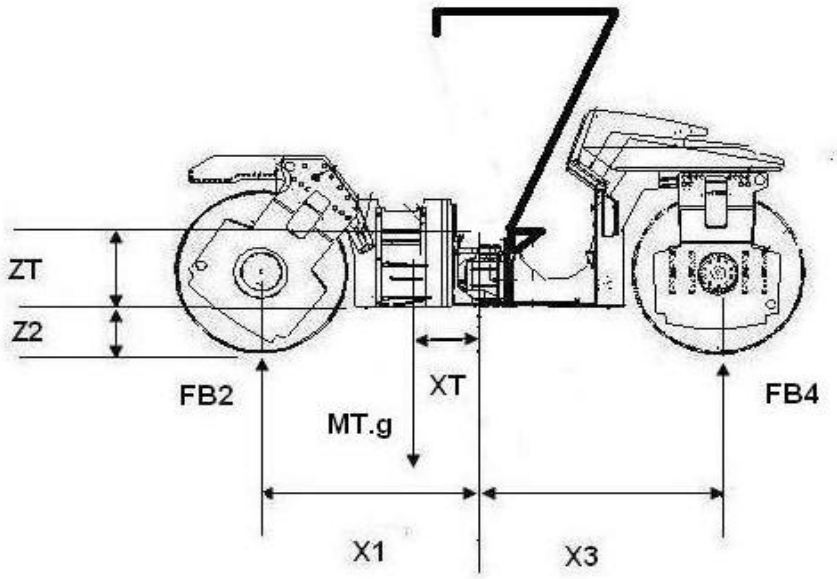

Figure3.2. Gravity load case.

To model this case a uniform gravitational acceleration was applied as a gravity force in z-direction downwards with standard value 1g ($9.81 m/s^2$) while the longitudinal and lateral acceleration kept as zero. The friction forces between the drums and ground were not applied in this case because the Asphalt Roller was considered standing on a ground level. Free body diagram, which is shown in figure 3.1 and 3.2, was helpful to find out the external normal reaction forces at points 1, 2, 9 and 10 respectively.

At y –axis of the external load points 9 and 10

$$\sum MY = 0 \tag{3.7}$$

$$FB_2 = \frac{\left[MT \cdot g \cdot \cos q \cdot (X_T + X_3) - MT \cdot g \cdot \sin q \cdot (Z_T + Z_2)\right]}{X_1 + X_3} \tag{3.8}$$

$$\sum FZ = 0 \tag{3.9}$$

$$FB_2 + FB_4 = MT \cdot g \cdot \cos q \qquad (3.10)$$

If the Asphalt Roller was assumed standing on an inclination surface uphill, the friction forces should be considered in that model as a full friction force between the ground and rear drum with a full coefficient of friction $\{h_R = 0.5\}$ in order to keep the Asphalt Roller from sliding back while the friction force between the ground and the front drum could be calculated from equilibrium equation:

$$FB_3 = h_R \cdot FB_4$$

$$\sum FX = 0$$

$$FB_1 + FB_3 = -MT \cdot g \cdot \sin q$$

3.3 Maximum torque load case

This case is important because it depicts the behaviour of an Asphalt Roller if it is working under special conditions like 'getting stuck' in a clay road. During the test the Asphalt Roller was welded to a fixed support simulating the affect of the above condition. Therefore a high maximum torque would be applied. To model this case and made it close to reality the Asphalt Roller was considered under gravity conditions and no rectilinear motion was assumed (no acceleration). Friction forces were not considered because of the drum slipping, but high maximum torque about y-axis was applied on the drive forks with value 15600(Nm) [4]. Free body diagram which shown in the figure 3.1 and 3.3 was useful to calculate the external forces at external load points 1, 2, 9 and 10.

At y-axis of the external load point 9 and 10

$$\sum MY = 0 \qquad (3.11)$$

$$FB_2 = \frac{[MT \cdot g \cdot \cos q \cdot (X_T + X_3) - MT \cdot g \cdot \sin q \cdot (Z_T + Z_2) - MY_2 - MY_{13}]}{X_1 + X_3}$$

(3.12)

$$\sum FZ = 0 \tag{3.13}$$

$$FB_2 + FB_4 = MT \cdot g \cdot \cos q \tag{3.14}$$

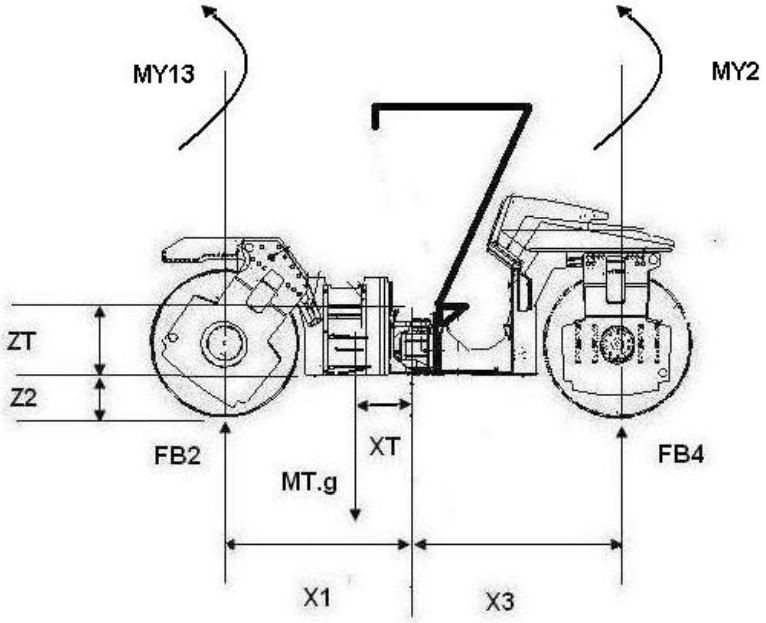

Figure3.3. Maximum torque load case.

3.4 Acceleration load case

According to the Newton's second law 'The acceleration or retardation of an object as produced by a net force which is directly proportional to the magnitude of the net force, in the same direction as the net force and inversely proportional to the mass of the object' In terms of an equation, the net force is equated to the product of the mass times the acceleration.

$$F_{NET} = mass \cdot A \tag{3.15}$$

$$F_{NET} = [F_X, F_Y, F_Z] \quad (3.16)$$

$$A = [A_X, A_Y, A_Z] \quad (3.17)$$

Where, F_{NET} is the net force vector (N) and A is acceleration vector (m/s^2). To model this case, it is to be assumed that the Asphalt Roller accelerates or decelerates when it is subjected to unbalanced force. The model was studied the deceleration case and it was assumed that the Asphalt Roller had rectilinear motion in x-direction with longitudinal standard acceleration (0.5g m/s^2) [4] and by considering the gravity acceleration as force:

$$\sum FX = mass \cdot A_X \quad (3.18)$$

$$\sum FY = 0 \quad (3.19)$$

$$\sum FZ = 0 \quad (3.20)$$

The braking forces were modelled un-symmetric because of using different reaction forces and same coefficient of friction for the front and rear drum with values $\{h_F = 0.5\}$and $\{h_R = 0.5\}$[4]. From the free body diagram shown in figure 3.1 and 3.4 the external reaction and longitudinal braking forces were calculated at points 1, 2, 9 and 10 respectively

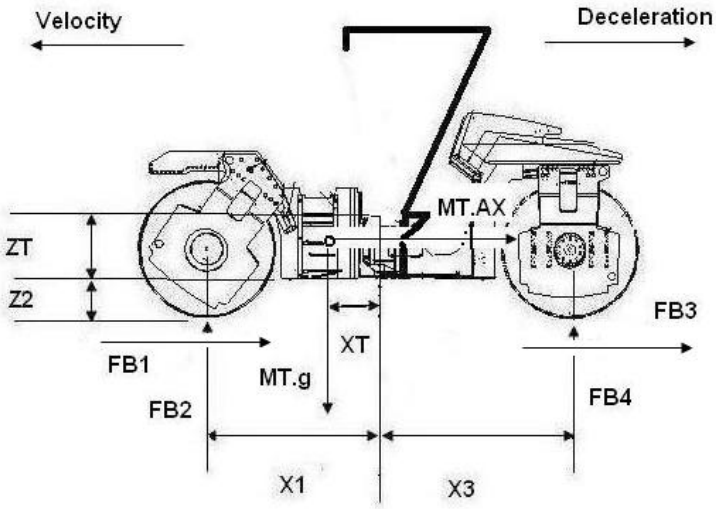

Figure3.4. Acceleration load case.

At y- axis for the external load points 9 and 10:

$$\sum MY = 0 \tag{3.21}$$

$$FB_2 = \frac{\left[MT \cdot g \cdot \cos q \cdot \left(X_T + X_3\right) - MT \cdot \left(g \cdot \sin q + A_X\right)\left(Z_T + Z_2\right)\right]}{X_1 + X_3}$$

(322)

$$\sum FZ = 0 \tag{3.23}$$

$$FB_2 + FB_4 = MT \cdot g \cdot \cos q \tag{3.24}$$

The braking forces

$$FB_1 = h_F \cdot FB_2 \tag{3.25}$$

$$FB_3 = h_R \cdot FB_4 \tag{3.26}$$

The moment at the centre of gravity for each rigid body is

$$\sum M_G = J \cdot a \tag{3.27}$$

And for an arbitrary point

$$\sum M_{POINT} = J \cdot a + mass \cdot A \cdot d \tag{3.28}$$

Where J is the moment of inertia (Kg.m^2), $a = \dot{w}$ is the angular acceleration (rad/s^2) and d is the distance between the gravity and any arbitrary point (m). Rigid bodies of the Asphalt Roller are assumed have a rectilinear translation which is defined as any motion in which every line in the body remains parallel to its original position at all times and there is no rotation of any of these lines namely, no angular acceleration $(\dot{w} = 0)$ [3]. So, the general equations for the plane motion become:

$$\sum M_G = 0 \tag{3.29}$$

$$\sum M_{POINT} = mass \cdot A \cdot d \tag{3.30}$$

The torque about y –axis at the drive forks was calculated by taking summation of torques about y-axis at the centre of the gravity of the drum:

$$\sum M_G Y = 0 \tag{3.31}$$

Where the torque applied at the drive side of the front drum

$$MY_2 = FB_1 \cdot R \tag{3.32}$$

The torque applied at the drive side of the rear drum

$$MY_{13} = FB_3 \cdot R \tag{3.33}$$

Where R is the radius of the drum (m)

3.5 Lifting load case

A lifting plate was used with a chain, steel wire or traps to lift the Asphalt Roller. Lifting eyelets were placed on each side of the Asphalt Roller and sometime there was one eyelet in the middle specially was used to lift the small Rollers. According to the design the lifting eyelets were not symmetric where the location of the front eyelets were placing before the centre of the front drum while the rear eyelets found after the centre of the rear drum and that gave unsymmetrical lifting loads between the front and rear body [5]. During lifting process the Steering Hitch was locked and the Steering Wheel was turned so that the machine was set to drive forward in order to prevent inadvertent turning before lifting the Asphalt Roller. Rectilinear motion in z-direction upward was assumed with standard vertical acceleration (1.6g m/s^2) including the Hoist factor [4] By applying Newton's second law and using the free body diagram shown in figure 3.5 the external lifting loads were calculated at points 3, 4,6 and 7 respectively.

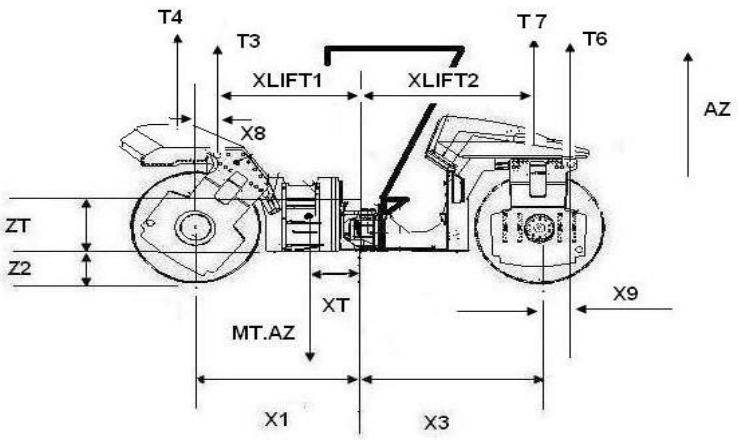

Figure 3.5.Lifting case.

At the centre of the gravity of the total mass of the Asphalt Roller

$$X_6 = X_{LIFT1} - X_T \tag{3.34}$$

$$X_7 = X_{LIFT2} + X_T \tag{3.35}$$

$$\sum MY = 0 \tag{3.36}$$

$$(T_3 + T_4) \cdot X_6 - (T_6 + T_7) \cdot X_7 = 0 \tag{3.37}$$

$$\sum FZ = mass \cdot A_Z \tag{3.38}$$

$$T_3 + T_4 + T_6 + T_7 = MT \cdot A_Z \tag{3.39}$$

$$T_3 = T_4 \tag{3.40}$$

$$T_6 = T_7 \tag{3.41}$$

3.6 Pulling load case

Trailers had many shapes and sizes. Pulling a trailer by using an Asphalt Roller was required extra care and attention because the trailer put extra weight on the Asphalt Roller and increased the space to drive and stop safely. Retrieval device was available in the Asphalt Roller to pull the trailer. Asphalt Roller was subjected to a longitudinal force during the pulling operation, which was calculated as capacity of the retrieval device (N). The capacity of the retrieval device was defined as a value of the force applied to a machine mounted retrieval device that results in a stress level equal to the yield strength of the material that was used to manufacture the retrieval device. The capacity of the pulling case should be equal to 1.5 times the trailer mass multiplied by the acceleration due to the gravity g $\left[F_{PULL} = 1.5 \cdot g \cdot M_{trailer}\right]$ which was considered as a longitudinal input force in the model [4]. If there was no retrieval device the longitudinal force would be calculated as the capacity of the eyelet itself. The pulling eyelet was placed at the yoke. In the verification a 5255 kg trailer mass was used. Constant speed was considered during pulling operation (no acceleration) after considering the gravitational acceleration as gravity force and a full friction force was applied at the rear drum with value $\{h_R = 0.5\}$ while the front one was calculated from the equilibrium equations according to Newton's first law. Free body diagram which is shown in figure 3.1 and 3.6 used to obtain the external forces at points 1,2,8,9 and 10.

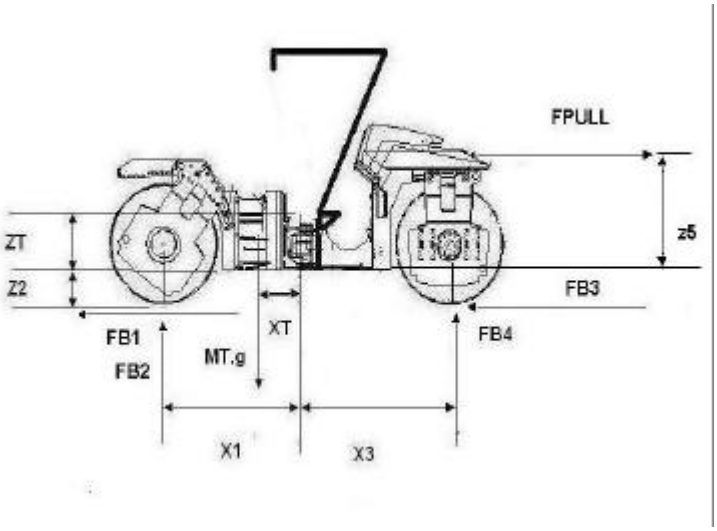

Figure3.6. Pulling load case.

At y-axis of the external points 9 and 10

$$\sum MY = 0 \tag{3.42}$$

$$FB_2 = \frac{\left[MT \cdot g \cdot \left(X_3 + X_T\right) \cdot \cos q\right]}{X_1 + X_3} - \frac{\left[F_{PULL} \cdot \left(Z_5 + Z_2\right) - MT \cdot g \cdot \sin q \cdot \left(Z_T + Z_2\right)\right]}{X_1 + X_3} \tag{3.43}$$

$$\sum FZ = 0 \tag{3.44}$$

$$FB_2 + FB_4 = MT \cdot g \cdot \cos q \tag{3.45}$$

Friction forces

$$FB_3 = h_R \cdot FB_4 \tag{3.46}$$

$$\sum FX = 0 \tag{3.47}$$

$$FB_1 + FB_3 = F_{PULL} + MT \cdot g \cdot \sin q \qquad (3.48)$$

3.7 Towing load case

This case arises when any other machine for transportation tries to tow an Asphalt Roller. Any Roller should be towed slowly, maximum 3 km/h and for a short distance only, maximum 300 meter. When an Asphalt Roller is towed, the towing retrieval device must be connected to the towing eyelet. The Asphalt Roller can be towed if it is subjected to an external axial force, which can be calculated as a capacity (N) of the retrieval device that should be equal to 1.5 times the Asphalt Roller mass multiplied by the acceleration due to the gravity g $\left[F_{TOWING} = 1.5 \cdot g \cdot MT\right]$which was considered as input force in the model [4]. The Asphalt Roller - mounted retrieval device can be at the front or rear body and it should be in location that is easily accessible for attaching a towrope, a chain or a tow bar. During towing an Asphalt Roller the drums should be rotated freely by disengaging the brakes. Equal values of the friction forces applied at the drums when the Asphalt Roller moving in constant speed (no acceleration) during the towing operation. Free body diagram shown in figure 3.7 was used to find the external forces acting at points 1,2,5,9 and 10 applying the Newton's first law.

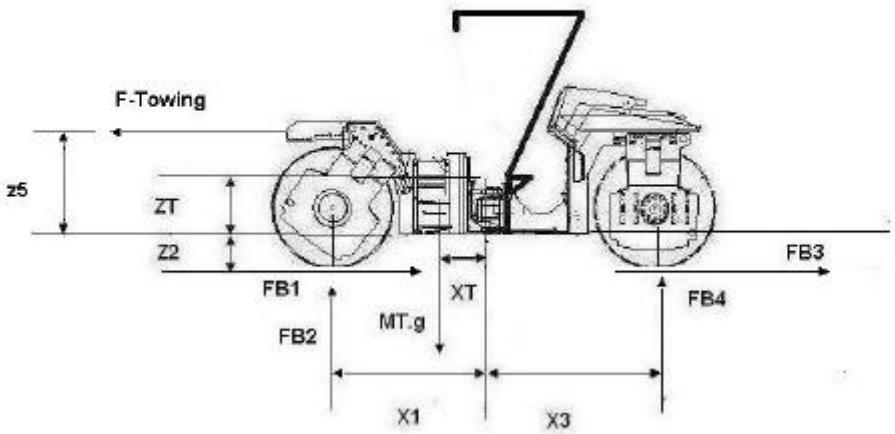

Figure3.7. Towing load case.

At y-axis of the external load points 9 and 10

$$\sum MY = 0 \tag{3.49}$$

$$FB_2 = \frac{\left[F_{TOWING} \cdot (Z_5 + Z_T) + MT \cdot g \cdot \cos\theta \cdot (X_T + X_3)\right]}{X_1 + X_3} - \frac{\left[MT \cdot g \cdot \sin\theta \cdot (Z_T + Z_2)\right]}{X_1 + X_3} \tag{3.50}$$

$$\sum FZ = 0 \tag{3.51}$$

$$FB_2 + FB_4 = MT \cdot g \cdot \cos\theta \tag{3.52}$$

The friction forces

$$\sum FX = 0 \tag{3.53}$$

$$FB_1 + FB_3 = F_{TOWING} - MT \cdot g \cdot \sin\theta \tag{3.54}$$

3.8 Steering load case (Gravity)

The design of the steering system has an influence on the directional response behaviour of a motor vehicle. The function of the steering system is to steer the front wheels in response to driver command inputs in order to provide overall directional control of the vehicle. The actual steer angles are affected by the geometry of the suspension system and the geometry and reactions within the steering system. In an Asphalt Roller the steering system or Steering Hitch which consists of two hydraulic cylinders as shown in figure 3.8. These cylinders created forces when the drum steers to the left or right under the gravity conditions according to the formula:

$$F_{CYLINDER} = P_{CYLINDERE} * A_{CYLINDER} \tag{3.55}$$

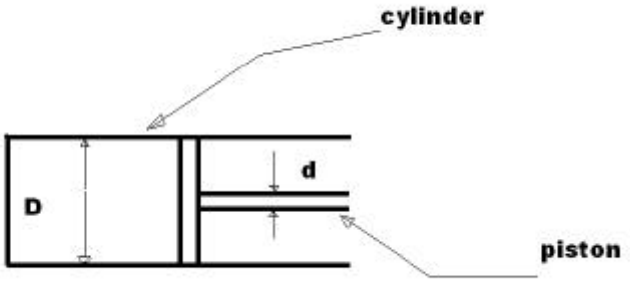

Figure .3.8. Hydraulic cylinder.

The first force acting on the area of the hydraulic cylinder A_1

$$F_1 = P \cdot A_1 \tag{3.56}$$

Where P is the pressure cylinder

$$A_1 = p\left[\frac{D}{2}\right]^2 \tag{3.57}$$

The second force

$$F_2 = P \cdot A \tag{3.58}$$

Where A is the difference in area between the cylinder and the piston

$$A = A_1 - A_2 \tag{3.59}$$

$$A = p\left(\frac{D}{2}\right)^2 - p\left(\frac{d}{2}\right)^2 \tag{3.60}$$

These forces create a moment in z-z direction at steering which shown in figure3.9

$$M_Z = \left(F_1 + F_2\right) \cdot Y \tag{3.61}$$

Where Y is the distance (m)

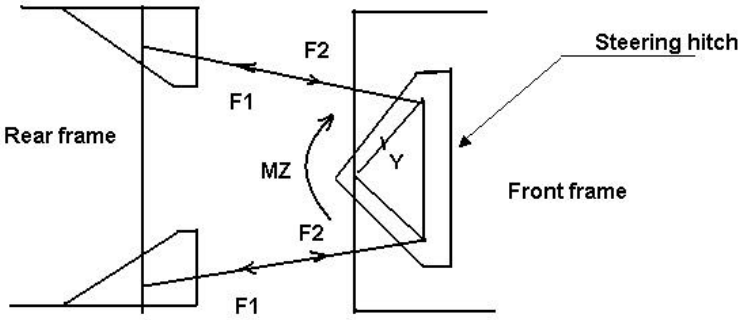

Figure3.9. Steering hitch with the forces of the hydraulic cylinders.

Under the same previous boundary conditions the external normal forces at load points 1, 2, 9 and 10 were calculated according to the figure 3.1 and 3.2. [6]:

At y-axis for external load points 9 and 10

$$\sum MY = 0 \tag{3.62}$$

$$FB_2 = \frac{\left[MT \cdot g \cdot \left(X_T + X_3\right)\right]}{X_1 + X_3} \tag{3.60}$$

$$\sum FZ = 0 \tag{3.63}$$

$$FB_2 + FB_4 = MT \cdot g \cdot \cos q \tag{3.64}$$

Three models were assumed to explain this case:

3.8.1 Fatigue load case (First model)

In this model the external loads acting on the drum which stands on a plane were assumed as distributed loads along the width of the drum as shown in the figure 3.10. The friction forces created moment in z-direction. No acceleration was used for this model after considering the

gravitational acceleration as gravity force and the coefficient of friction with the value 0.5 was used [4].

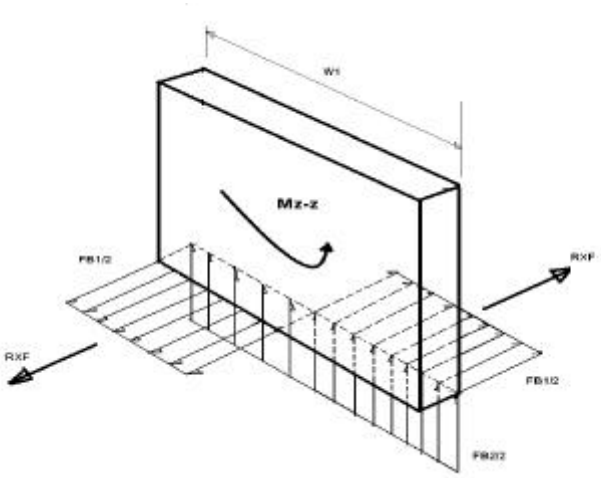

Figure3.10. Fatigue load case model.

The moment in z-z axis, which is shown in the figure 3.11, was calculated according to the equations:

$$RX_F = \frac{FB_1}{2} \cdot \frac{W_1}{2} \tag{3.65}$$

$$\frac{FB_1}{2} = h_F \cdot \frac{FB_2}{2} \tag{3.66}$$

For the rear drum the resultant

$$RX_R = \frac{FB_3}{2} \cdot \frac{W_1}{2} \tag{3.67}$$

$$\frac{FB_3}{2} = h_R \cdot \frac{FB_4}{2} \tag{3.68}$$

For the front drum at a-axis

$$MZ_1 = h_F \cdot \frac{FB_2}{2} \cdot \frac{W_1}{2} \cdot \frac{W_1}{4} + h_F \cdot \frac{FB_2}{2} \cdot \frac{W_1}{2} \cdot \frac{W_1}{4} \tag{3.69}$$

For the rear drum

$$MZ_2 = h_R \cdot \frac{FB_4}{2} \cdot \frac{W_1}{4} + h_R \cdot \frac{FB_4}{2} \cdot \frac{W_1}{2} \cdot \frac{W_1}{4} \qquad (3.70)$$

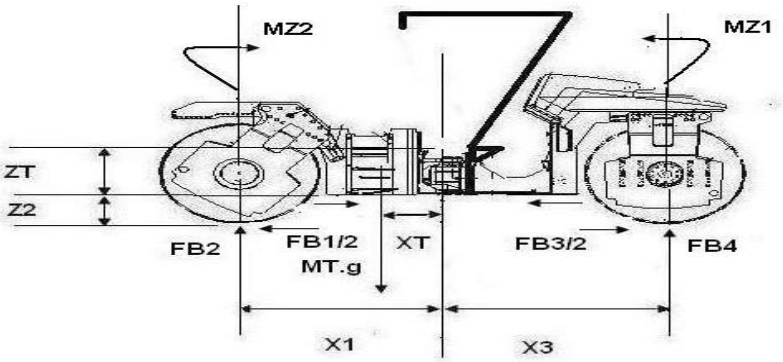

Figure3.11. Steering gravity case.

3.8.2 Maximum load case (second model)

The assumption which shown in the figure 3.12 considers the drum stands on a concave surface namely the drum contact the ground at the edges only

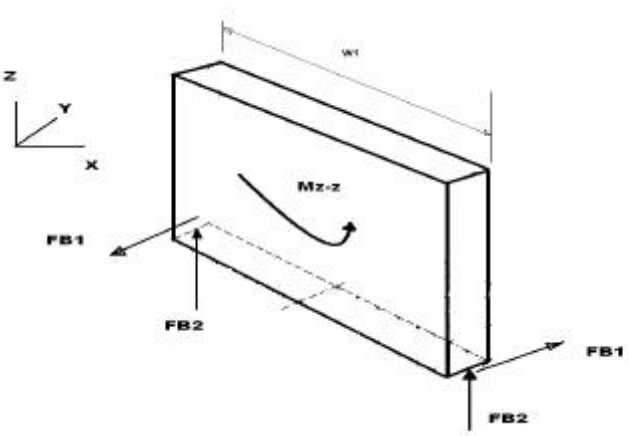

Figure3.12. Maximum load case model.

The same procedure was used to calculate the external reaction forces but the moment about z-axis for the front drum was different [4]

Front drum

$$MZ_1 = h_F \cdot \frac{FB_2}{2} \cdot \frac{W_1}{2} + h_F \cdot \frac{FB_2}{2} \cdot \frac{W_1}{2} \tag{3.71}$$

The friction force

$$\frac{FB_1}{2} = h_F \cdot \frac{FB_2}{2} \tag{3.72}$$

Rear drum

$$\frac{FB_3}{2} = h_R \cdot \frac{FB_4}{2} \tag{3.73}$$

$$MZ_2 = h_R \cdot \frac{FB_4}{2} \cdot \frac{W_1}{2} + h_R \cdot \frac{FB_4}{2} \cdot \frac{W_1}{2} \tag{3.74}$$

3.8.3. Maximum input load case (third model)

The assumption in this model considered the drum stands on a concave surface and a maximum torque which produced from the hydraulic cylinders, was applied as input torque with value (40000N.m) at the steering hitch [4]. The external reaction forces were calculated as before and according to the free body diagram in figure3.10.

$$MZ = 40000 \tag{3.75}$$

$$FB_1 = \frac{MZ}{W_1} \tag{3.76}$$

$$FB_3 = \frac{MZ}{W_1} \tag{3.77}$$

3.9 Steering lateral acceleration case

In this case the roller was supposed to be moving along plane curvilinear path with a constant values v = 11 KMPH, R_1 = 7690mm and R_2 =5560 mm [4]

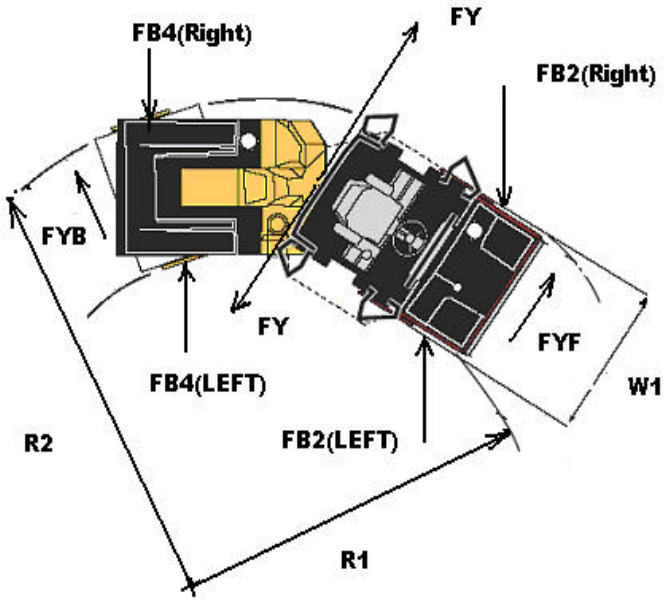

Figure3.12. Lateral acceleration case.

Where v is the constant velocity (Km/Hr), *R_1 and R_2 is the inner and outer* turning radius respectively.

The average value of the inner and outer turning radius was calculated:

$$R = \frac{R1 + R2}{2} = 6.625m \tag{3.78}$$

When the Asphalt Roller was considered moving with constant speed, namely the longitudinal acceleration set to zero. Lateral acceleration calculated according to the relation:

$$A_Y = \frac{v^2}{R} = \frac{\left(\frac{11}{3.6}\right)^2}{6.625} = 1.409 m/s^2 \quad (3.79)$$

Where A_Y is the lateral acceleration (m/s^2),

Hence in order to made the Asphalt Roller mass move with uniform velocity it was necessary that the Asphalt Roller mass was to be subjected to a force which produced that lateral acceleration towards the center of motion (rotation). This force was called the centripetal force (N). It could be defined as the necessary force to be applied on the Asphalt Roller towards the center of rotation and it was calculated according to the Newton's second law:

$$\sum FY = mass \cdot A_Y \quad (3.80)$$

$$FY = MT \cdot A_Y \quad (3.81)$$

$$FY = 18243N \quad (3.82)$$

This force was balanced by an equal and opposite force due to the inertia of the Asphalt Roller mass in order to keep it at a constant distance from the center of motion, which is shown in the figure3.12. That force was called the centrifugal force, which was always directed, away from the center of the motion. [7]. Therefore, the Asphalt Roller was subjected to a centrifugal force and the lateral friction forces on each drum will resist this force and they were supplied the necessary centripetal force. Because of the lateral forces and that curvature road the normal external reaction forces wouldn't distribute equally at each side of the drum

The external and internal forces calculated by using the previous second model, which was considered the drums stand at a concave surface, and the connection would be at the drum edge only. From the free body diagram of the figure 3.12 the unequal external forces were calculated as in equations 3.82-3.85:

$$FZ_{LEFT} = FB_{2LEFT} + FB_{4LEFT} \quad (3.82)$$

$$FZ_{RIGHT} = FB_{2RIGHT} + FB_{4RIGHT} \quad (3.83)$$

$$FB_2 = FB_{2LEFT} + FB_{2RIGHT} \tag{3.84}$$

$$FB_4 = FB_{4LEFT} + FB_{4RIGHT} \tag{3.85}$$

From the moment about x-x axis for the right side of the Asphalt Roller the left forces were calculated:

$$FZ_{LEFT} = \frac{[MT \cdot g \cdot (Y_T + 0.5 \cdot W_1) \cdot \cos q]}{W_1} - \frac{[MT \cdot (Z_T + Z_2) \cdot A]}{W_1} \tag{3.86}$$

$$\sum FZ = 0 \tag{3.87}$$

$$FZ_{RIGHT} = MT \cdot g \cdot \cos q - FZ_{LEFT} \tag{3.88}$$

The resultant external normal forces were calculated by taking the moment at the contact between rear drum and the ground namely, the external load points 9 and 10:

$$\sum MY = 0 \tag{3.89}$$

$$FB_2 = \frac{[MT \cdot g \cdot (X_T + X_3) \cdot \cos q - MT \cdot g \cdot (Z_T + Z_2) \cdot \sin q]}{X_1 + X_3} \tag{3.90}$$

$$\sum FZ = 0 \tag{3.91}$$

$$FB_2 + FB_4 = MT \cdot g \cdot \cos q \tag{3.92}$$

$$FY = FYF + FYB \tag{3.93}$$

For the front drum

$$\sum MX = 0 \tag{3.94}$$

$$MZ = MR \cdot A_Y \cdot (X_B + X_1) + MF \cdot A_Y \cdot X_4 + MD_2 \cdot A_Y \cdot X_2 - FYF \cdot X_2 \tag{3.95}$$

For the rear drum

$$MX = \left[\frac{FZ_{RIGHT}}{2} \cdot \frac{W_1}{2} - \frac{FZ_{LEFT}}{2} \cdot \frac{W_1}{2} \right] - FYB \cdot R \qquad (3.96)$$

$$MZ = MF \cdot A_Y \cdot \left(X_A + X_3 \right) + MR \cdot A_Y \cdot X_5 + MD_1 \cdot A_Y \cdot X_2 - FYB \cdot X_2 \qquad (3.98)$$

4 Theoretical Model in MATLAB®

One of the goals of this work is to get knowledge about static and quasi-static load calculations for different cases which are approved by building a mathematical model in MATLAB®. It can be predicted the internal element forces, external forces and their corresponding moments in 3D at specified load points. Firstly the Asphalt Roller split at the steering hitch to get the forces and moments by assuming four rigid bodies (front Roller mass MF, rear Roller mass MR, front drum mass MD_1 and the rear drum mass MD_2). After that a front sections A-A was used to cut the mass MF and two rear sections B-B and C-C were used to cut the mass MR respectively. Finally the Asphalt Roller was specified as eleven rigid bodies:

- Front drum mass MD_1.
- Front vibrated fork mass MVF.
- Front drive Fork mass MDF.
- First front mass section.
- Second front mass section MS.
- First rear mass section MK.
- Second rear mass section MH.
- Yoke mass.
- Rear vibrated fork MVFB.
- Rear drive fork MDFB.
- Rear drum mass MD_2.

4.1 Vibrated fork

There were two vibrated forks in the Asphalt Roller which were placed in opposite directions. These forks were used to join the drum with frame and to transfer the forces and moments to other parts of the Asphalt Roller. A vibration motor was mounted on the vibrated forks side. The geometry of the front fork was differed from the rear one and they were consisted of four rubber elements, which had square

geometry and they were modelled as linear and rotational springs with same physical properties. Internal load points 3 and 10 have been chosen at the connection between the fork and the frame. The location of the centre of gravity and the load points were known from the available vibrated fork model (figure 4.5)

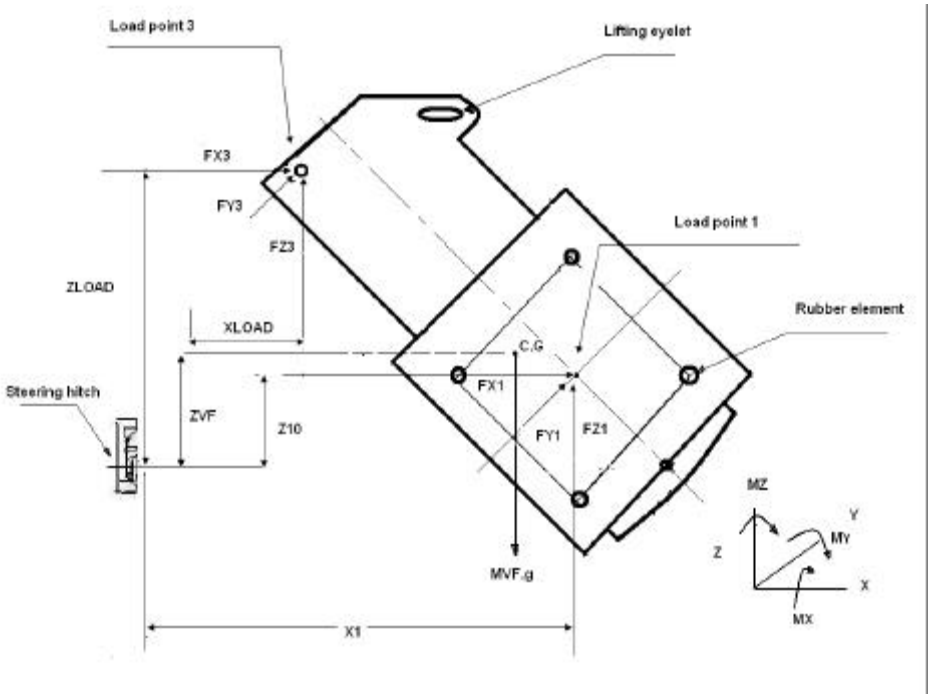

Figure 4.1.Front vibrated fork.

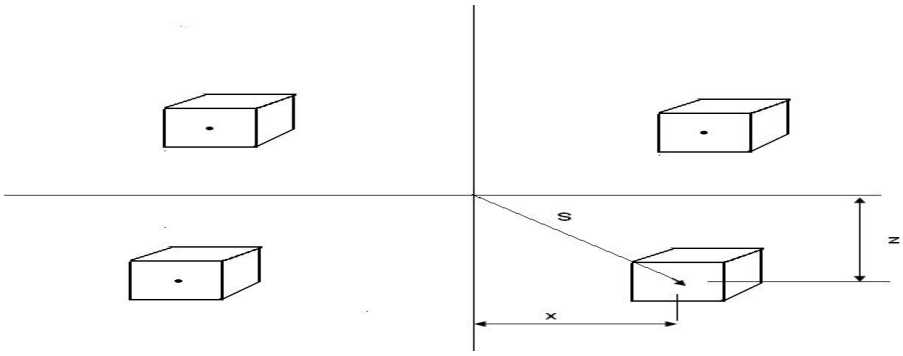

Figure4.2. The Rubber elements geometry of the vibrated fork.

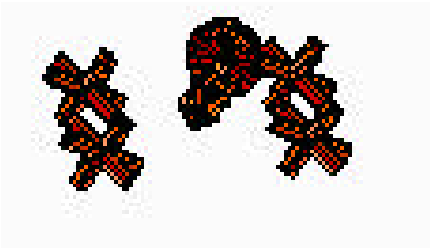

Figure 4.3. Available geometry of the rubber

The rubber elements were modelled as two types of spring in 3D, which defined as linear translation, and rotation type. The first type was known value but the second type was calculated according to the geometry and the number of the rubber elements. By considering super translation and rotation springs in3D were placed in the centre of the square where:

$$KX_1 = 4 \cdot K_{SHEAR}$$

$$KY_1 = 4 \cdot K_{AXIAL}$$

$$KZ_1 = 4 \cdot K_{SHEAR}$$

Where K_{SHEAR} =390000 N/m, K_{AXIAL}=3300000 N/m.

KX_1 and KZ_1 is the super linear translation shear stiffness, KY1 is the super linear translation axial stiffness. From the geometry showed in figure 4.2 and 4.3 the rotational stiffness could be derived as

$$\sum M_{Z-Z} = \sum_{N=1}^{4} K_{AXIAL} \cdot X^2 \cdot \Delta f \qquad (4.1)$$

$$KCZ_1 = \frac{\sum M_{Z-Z}}{\Delta f} = 1.14873E + 6 \frac{N.m}{rad} \qquad (4.2)$$

$$\sum M_{X-X} = \sum_{N=1}^{4} K_{AXIAL} \cdot Z^2 \cdot \Delta f \qquad (4.3)$$

$$KCX_1 = \frac{\sum M_{X-X}}{\Delta f} = 126773 \frac{N.m}{rad} \qquad (4.4)$$

$$\sum M_{Y-Y} = \sum_{N=1}^{4} K_{SHEAR} \cdot S^2 \cdot \Delta f \tag{4.5}$$

$$KCY_1 = \frac{\sum M_{Y-Y}}{\Delta f} = 149916 \frac{N.m}{rad} \tag{4.6}$$

Where the distances X=0.295, Z=0.098 m, KCX_1 is super rotational stiffness in x-axis, KCY1 is super rotational stiffness in y-axis and KCZ_1 is super rotational stiffness in z-axis [8].

The general equations, which were governing static and quasi-static loads, were used to compute the forces according to the free body diagram in the figure 4.1 and 4.4.

$$\sum FX = mass \cdot A_X \tag{4.7}$$

$$FX_3 = FX_1 + MVF \cdot g \cdot \sin q - MVF \cdot A_X \tag{4.8}$$

$$FX_{10} = FX_{13} + MVFB \cdot g \cdot \sin q - MVFB \cdot A_X \tag{4.9}$$

$$\sum FZ = 0 \tag{4.10}$$

$$FZ_3 = FZ_1 - MVF \cdot g \cdot \cos q \tag{4.11}$$

$$FZ_{13} = FZ_{12} - MVFB \cdot g \cdot \cos q \tag{4.12}$$

$$\sum FY = mass \cdot A_Y \tag{4.13}$$

$$FY_3 = FY_1 - MVF \cdot A_Y \tag{4.14}$$

$$FY_{10} = FY_{12} - MVFB \cdot A_Y \tag{4.15}$$

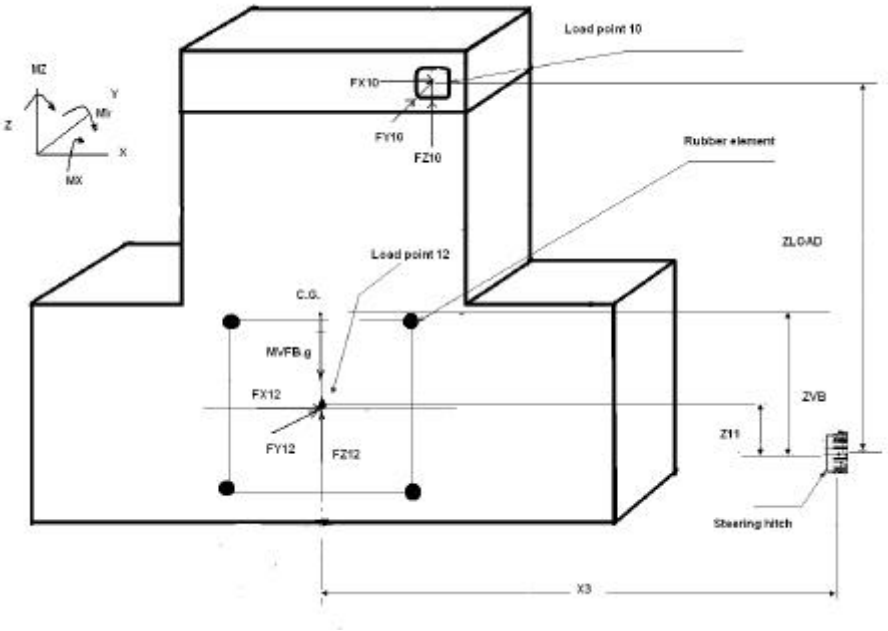

Figure 4.4. Rear vibrated fork.

$$\sum MX = 0 \tag{4.16}$$

At internal load point 3

$$\begin{aligned} MX_3 = {} & FZ_1 \cdot (Y_{LOAD} - Y_{100}) - MVF \cdot g \cdot (Y_{LOAD} - Y_{VF}) \cdot \cos q \\ & + FY_1 \cdot (Z_{LOAD} - Z_{10}) - MVF \cdot A_Y \cdot (Z_{LOAD} - Z_{VF}) + MX_1 \end{aligned} \tag{4.17}$$

At internal load point 10

$$\begin{aligned} MX_{10} = {} & FZ_{12} \cdot (Y_{LOAD} - Y_{100}) - MVFBg \cdot (Y_{LOAD} - Y_{VB}) \cdot \cos q \\ & + FY_{12} \cdot (Z_{LOAD} - Z_{11}) - MVFBA_Y (Z_{LOAD} - Z_{DR}) - MX_{12} \end{aligned} \tag{4.18}$$

$$\sum MY = 0 \tag{4.19}$$

At internal load point 3

$$\begin{aligned} MY_3 = {} & FZ_1 \cdot (X_1 - X_{LOAD}) - MVF \cdot g \cdot (X_{VF} - X_{LOAD}) \cdot \cos q + \\ & MVF \cdot [g \cdot \sin q - A_X] \cdot (Z_{LOAD} - Z_{VF}) + FX_1 \cdot (Z_{LOAD} - Z_{10}) \end{aligned} \tag{4.20}$$

At internal load point 10

$$MY_{10} = FZ_{12} \cdot (X_3 - X_{LOAD}) - MVFB \cdot g \cdot (X_{VR} - X_{LOAD}) \cdot \cos q + MVFB \cdot [g \cdot \sin q - A_X] \cdot (Z_{LOAD} - Z_{DR}) + FX_{12} \cdot (Z_{LOAD} - Z_{11}) \quad (4.21)$$

$$\sum MZ = 0 \quad (4.22)$$

At internal load point 3

$$MZ_3 = MVF \cdot A_Y \cdot (X_{VF} - X_{LOAD}) - FY_1 \cdot (X_1 - X_{LOAD}) \quad (4.23)$$

At internal load point 10

$$MZ_{10} = MVFB \cdot A_Y \cdot (X_{VR} - X_{LOAD}) - FY_{12} \cdot (X_3 - X_{LOAD}) \quad (4.24)$$

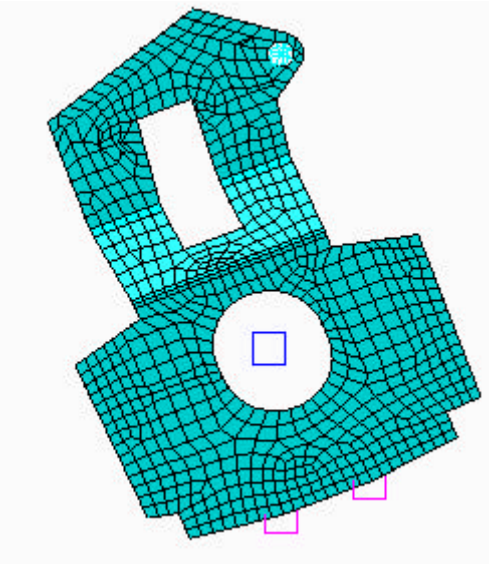

Figure 4.5. Available vibrated fork model.

4.2 Drive fork

There were two drive forks in an Asphalt Roller which were placed in opposite directions. The geometry of the front drive was differed from

the rear one and they were consisted of eight rubber elements, which modelled as rotational and linear translation springs with same physical properties. The drive motor was mounted on that side of fork. Internal load points 4 and 2 were limited at the contact surface between the fork and the frame to calculate the force and moments in 3D namely 6 DOF. The free body diagram in figure 4.6 and 4.9 is showed the locations and the dimensions of the forces and the load points according to the available driver fork in the figure 4.10

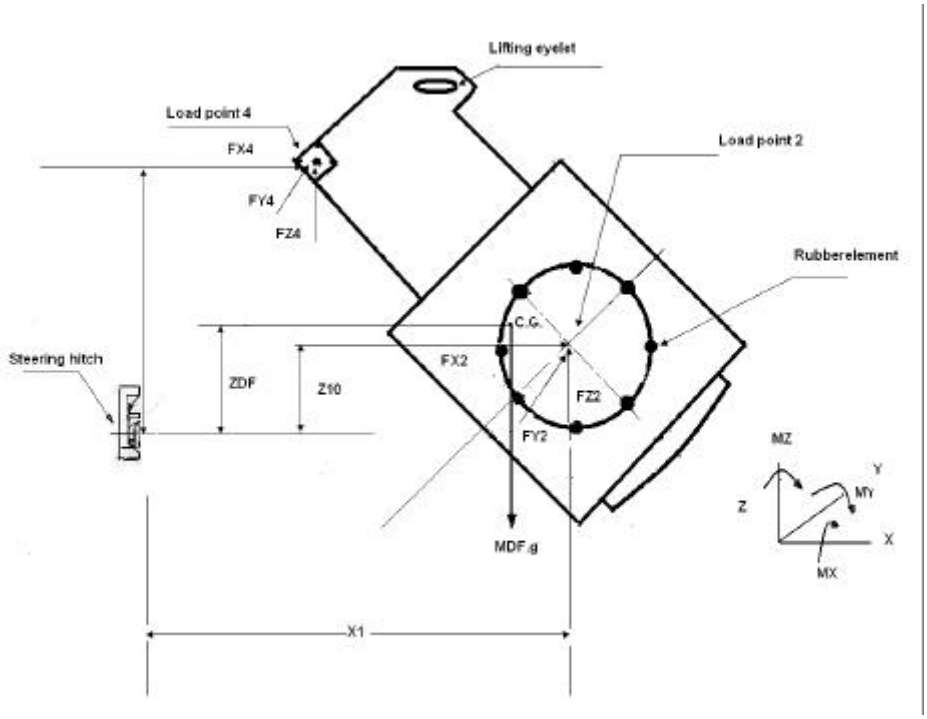

Figure 4.6. Front drive fork.

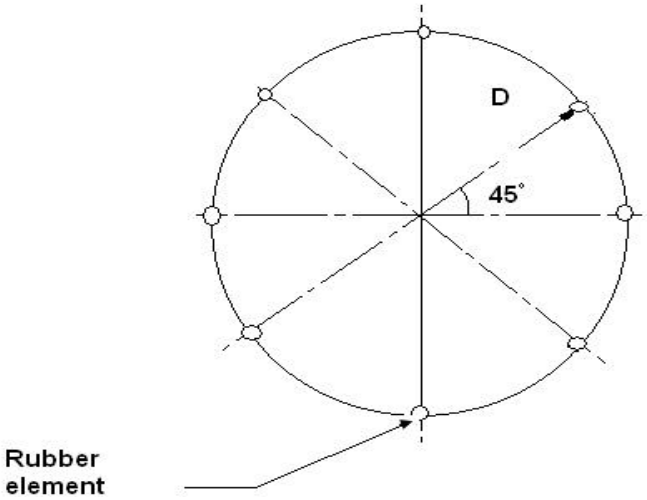

Figure 4.7. The geometry of the rubber elements of the drive fork.

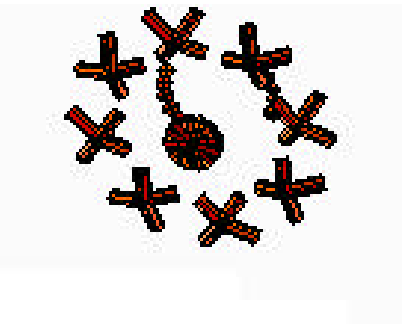

Figure 4.8. Available geometry of the rubber.

The rubber elements were modelled as two types of springs in 3D, which defined as translation, and rotation type. The first type was known value but the second type was calculated according to an assumption, which considered a circular geometry of the rubbers. Two of them were placed on the x-axis and another two elements placed on z-axis while other rubbers were distributed in axes had the inclination 45° as shown in figure 4.7 and 4.8. That assumption was considered super translation and rotation springs in 3D placed in the centre of the circle according to the number of rubber elements where:

$$KX_2 = 8 \cdot K_{SHEAR}$$

$$KY_2 = 8 \cdot K_{AXIAL}$$

$$KZ_2 = 8 \cdot K_{SHEAR}$$

Where K_{SHEAR} =390000 N/m, K_{AXIAL}=3300000 N/m.

KX_2 and KZ_2 is the super linear translation shear stiffness, KY2 is the super linear translation axial stiffness. The rotational stiffness was calculated by taking the moment at the centre of the circle [10].

$$\sum M_{Z-Z} = \sum_{N=1}^{4} K_{AXIAL} \cdot \frac{D}{\sqrt{2}} \cdot \frac{D}{\sqrt{2}} \cdot \Delta f + \sum_{N=1}^{2} K_{AXIAL} \cdot D^2 \cdot \Delta f \tag{4.25}$$

$$KCZ_2 = \frac{\sum M_{Z-Z}}{\Delta f} = 1.6917E + 6 \frac{N.m}{rad} \tag{4.26}$$

$$\sum M_{X-X} = \sum M_{Z-Z} \tag{4.27}$$

$$KCX_2 = KCZ_2 \tag{4.28}$$

$$\sum M_{Y-Y} = \sum_{N=1}^{8} K_{SHEAR} \cdot D^2 \cdot \Delta f \tag{4.29}$$

$$KCY_2 = \frac{\sum M_{Y-Y}}{\Delta f} = 399872 \frac{N.m}{rad} \tag{4.30}$$

Where KCX_2 is the super rotational stiffness in x-axis, KCY2 is super rotational stiffness in y-axis, KCZ_2 is super rotational stiffness in z-axis and D = 0.358 is the radius of the circle.

The general equation, which governs static and quasi-static load, used to compute the forces

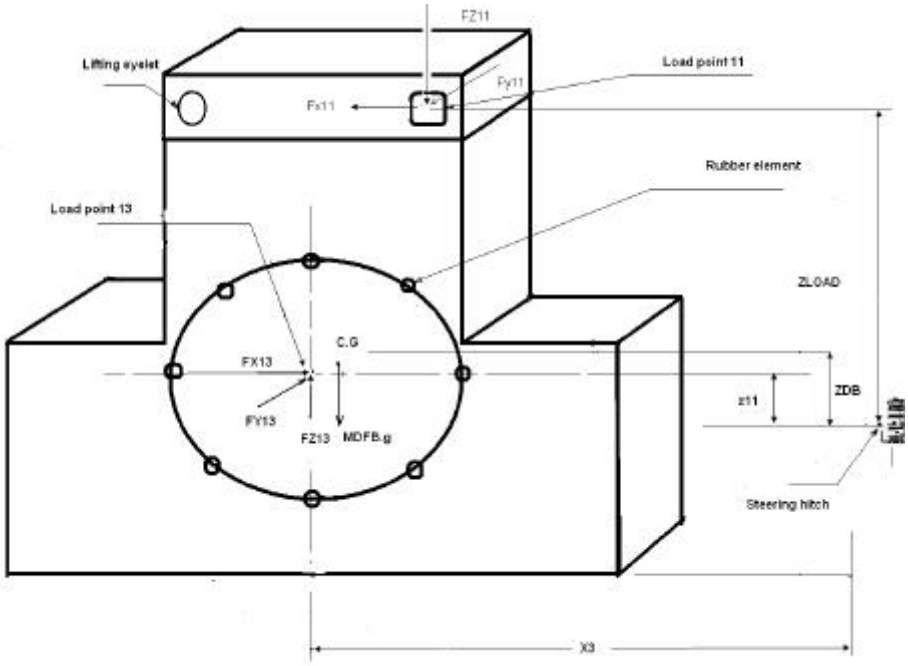

Figure 4.9. Rear drive fork

$$\sum FX = mass \cdot A_X \tag{4.31}$$

$$FX_4 = FX_2 + MDF \cdot g \cdot \sin q - MDF \cdot A_X \tag{4.32}$$

$$FX_{11} = FX_{13} + MDFB \cdot g \cdot \sin q - MDFB \cdot A_X \tag{4.33}$$

$$\sum FZ = 0 \tag{4-34}$$

$$FZ_4 = FZ_2 - MDF \cdot g \cdot \cos q \tag{4.35}$$

$$FZ_{11} = FZ_{13} - MDFB \cdot g \cdot \cos q \tag{4.36}$$

$$\sum FY = 0 \tag{4.37}$$

$$FY_4 = FY_2 - MDF \cdot A_Y \tag{4.38}$$

$$FY_{11} = FY_{13} - MDFB \cdot A_Y \tag{4.39}$$

$$\sum MX = 0 \tag{4.40}$$

At internal load point 4

$$\begin{aligned} MX_4 = {} & FZ_2 \cdot (Y_{LOAD} - Y_{200}) - MDF \cdot g \cdot (Y_{LOAD} - Y_{DF}) \cdot \cos q \\ & - FY_2 \cdot (Z_{LOAD} - Z_{10}) - MDF \cdot A_Y \cdot (Z_{LOAD} - Z_{DF}) + MX_2 \end{aligned} \tag{4.41}$$

At internal load point 11

$$\begin{aligned} MX_{11} = {} & FZ_{13} \cdot (Y_{LOAD} - Y_{200}) - MDFB\, g \cdot (Y_{LOAD} - Y_{DB}) \cdot \cos q \\ & + FY_{13} \cdot (Z_{LOAD} - Z_{11}) + MDFB\, A_Y \cdot (Z_{LOAD} - Z_{VR}) + MX_{13} \end{aligned} \tag{4.42}$$

$$\sum MY = 0 \tag{4.43}$$

At internal load point 4

$$\begin{aligned} MY_4 = {} & FZ_2 \cdot (X_1 - X_{LOAD}) - MDF \cdot g \cdot (X_{DF} - X_{LOAD}) \cdot \cos q \\ & + MDF \cdot [g \cdot \sin q - A_X] \cdot (Z_{LOAD} - Z_{DF}) + FX_2 \cdot (Z_{LOAD} - Z_{10}) - MY_2 \end{aligned} \tag{4.44}$$

At internal load point 11

$$\begin{aligned} MY_{11} = {} & FZ_{13} \cdot (X_3 - X_{LOAD}) - MDFB\, g \cdot (X_{DR} - X_{LOAD}) \cdot \cos q \\ & + MDFB\, [g \cdot \sin q - A_X] \cdot (Z_{LOAD} - Z_{DR}) + FX_{13} \cdot (Z_{LOAD} - Z_{11}) + MY_{13} \end{aligned} \tag{4.45}$$

$$\sum MZ = 0 \tag{4.46}$$

At internal load point 4

$$MZ_4 = MDF \cdot A_Y \cdot (X_{DF} - X_{LOAD}) + FY_2 \cdot (X_1 - X_{LOAD}) \tag{4.47}$$

At internal load point 11

$$MZ_{11} = MDFB\, A_Y \cdot (X_{DR} - X_{LOAD}) + FY_{13} \cdot (X_3 - X_{LOAD}) \tag{4.48}$$

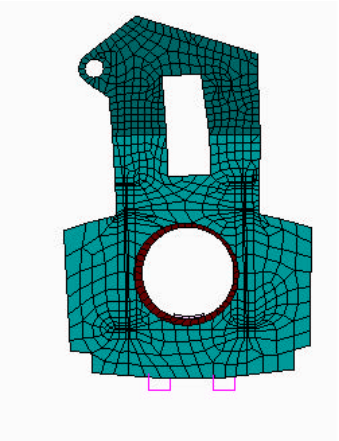

Figure 4.10. Available drive fork model.

4.3 Drum forces

The drum is a rotating cylindrical member used to transmit compaction forces to soil or other surface materials. The drum consisted of Spherical roller bearings, bearing Housings, Drum shell, Drum Heads and eccentric shaft for the vibration requirements. All these components were considered as a one single mass. The forces at the interface between the drums and the road can determine the movements of the Asphalt Roller. There were two assumptions to calculate the longitudinal and normal forces in the drum suspension:

- The first assumption by using the equilibrium equations and Newton's first and second law without considering about the torsion moments act on the rubber elements.
- The second assumption by using static coupling and virtual work done methods which were depending on the equilibrium equations in order to calculate the internal forces and moments at each edge of the drum according to the stiffness matrix and the resultant external forces and moments at the centre of the drum [9].

The geometry of the drum was not symmetric. Figure 4.11 and 4.12 shows the free body diagram of the drums with the external load points 1, 2, 9 and 10 and internal load points 1,2,12 and 13 respectively. The location of the centre of gravity with the mass and all dimensions

measured from the available drum model which shown in the figure4.13.

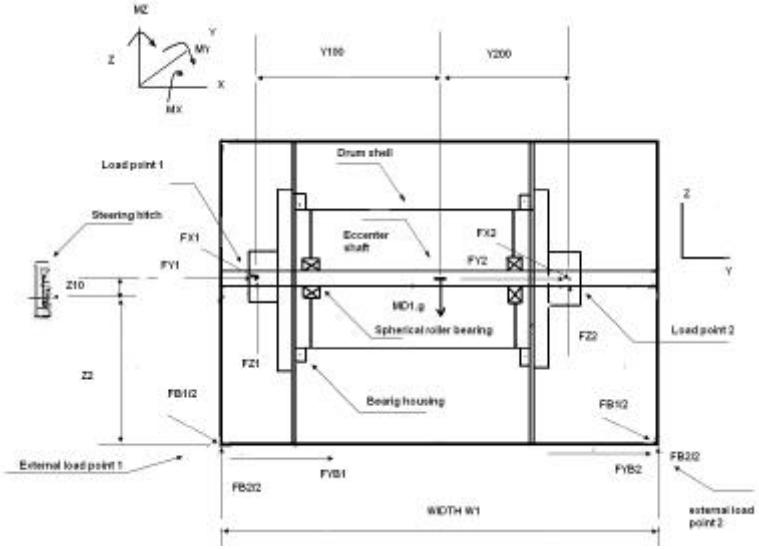

Figure 4.11. Front drum parts.

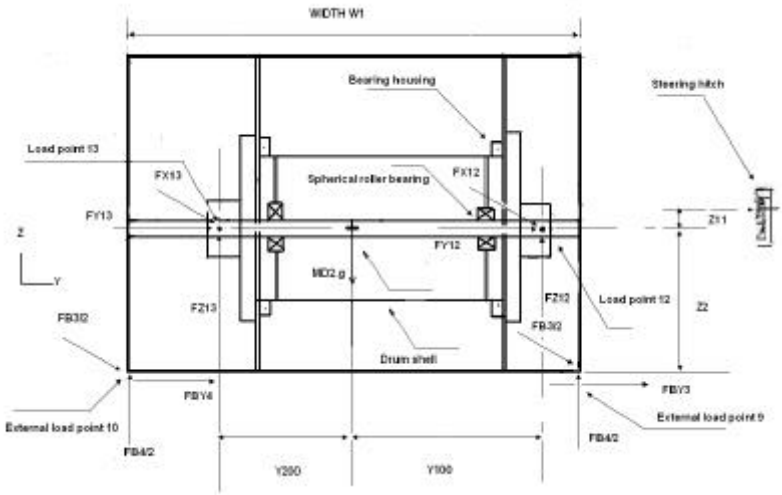

Figure 4.12. Rear drum parts.

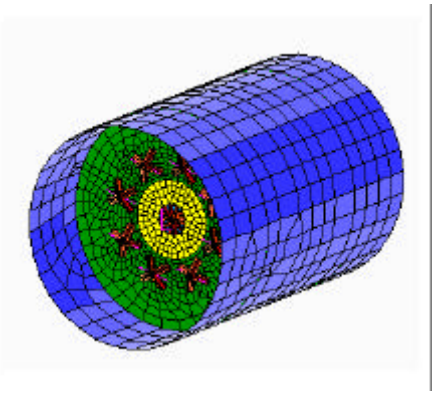

Figure 4.13. Available drum model.

In the first assumption the longitudinal element forces of the front drum were calculated according to the free body diagram, which is shown in the figure 4.11 and 4.12 by taking the summation of forces, and moments in x-x and z-z coordinate respectively:

$$\sum FX = mass \cdot A_X \tag{4.49}$$

$$FX_1 + FX_2 - FB_1 + MD_1 \cdot g \cdot \sin q = MD_1 \cdot A_X \tag{4.50}$$

At the centre of the drum

$$\sum MZ = 0 \tag{4.51}$$

$$FX_1 \cdot Y_{100} - FX_2 \cdot Y_{200} = 0 \tag{4.52}$$

Normal element forces were calculated by taking the summation of the forces and corresponding moments in z-z and x-x coordinate respectively:

$$\sum FZ = 0 \tag{4.53}$$

$$FZ_1 + FZ_2 + MD_1 \cdot g \cdot \cos q - FB_2 = 0 \tag{4.54}$$

At the external load point 2

$$MX = 0 \tag{4.55}$$

$$FZ_1 \cdot \left(Y_{100} + \frac{W_1}{2} \right) + FZ_2 \cdot \left(\frac{W_1}{2} - Y_{200} \right) - \frac{FB_2}{2} \cdot W_1 + MD_1 \cdot g \cdot \cos q \cdot \frac{W_1}{2} = 0 \tag{4.56}$$

The same procedure was used to calculate the normal and longitudinal element forces FX_{12}, FX_{13}, FZ_{12} and FZ_{13} respectively for the rear drum by using the rear drum mass MD_2 and the external force FB_4 and FB_3 instead. By using the second assumption the deflection in the z-direction was calculated at each side of the drum. The drum was described as a rigid bar with its centre of mass not coinciding with its geometric centre, i.e. $Y_{100} \neq Y_{200}$. This rigid bar was suspended by linear translation and rotational springs from each side. Each of the two coordinates was necessary to describe the rigid bar motion, displacements, Stiffness forces and moments. The choice of coordinates defined the type of coupling. The stiffness matrix was non-diagonal hence a static coupling existed. The equations of motion indicate static coupling, which is shown in the figure 4.14 and 4.15.

$$MD_1 \cdot \ddot{Z} + (KZ_1 + KZ_2) \cdot Z + (KZ_2 \cdot Y_{200} - KZ_1 \cdot Y_{100}) \cdot j_X = F_Z \tag{4.57}$$

$$\begin{aligned} &J\ddot{j} + (KZ_2 \cdot Y_{200} - KZ_1 \cdot Y_{100}) \cdot Z \\ &+ \left[KZ_1 \cdot Y_{100}^2 + KZ_2 \cdot Y_{200}^2 + KCX_1 + KCX_2 \right] \cdot j_X = MX \end{aligned} \tag{4.58}$$

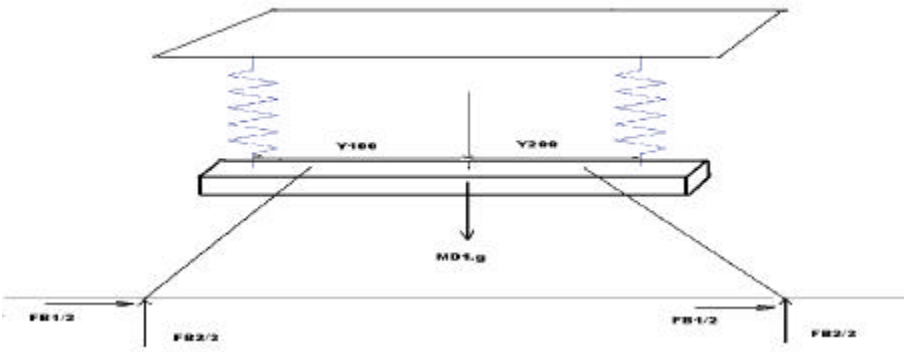

Figure4.14.Drum suspension

:

Normal reaction forces

$$FZ = \frac{FB_2}{2} + \frac{FB_2}{2} \tag{4.59}$$

Normal acceleration

$$\ddot{Z} = g \tag{4.60}$$

$$R_Z = FZ - MD_1 \cdot g \tag{4.61}$$

At the centre of the drum

$$MX = \frac{FB_2}{2} \cdot \frac{W_1}{2} - \frac{FB_2}{2} \cdot \frac{W_1}{2} \tag{4.62}$$

The moments of inertia is zero and the matrix equation can be written

$$\begin{bmatrix} KZ_1 + KZ_2 & KZ_2 \cdot Y_{200} - KZ_1 \cdot Y_{100} \\ KZ_2 \cdot Y_{200} - KZ_1 \cdot Y_{100} & KZ_1 \cdot Y_{100}^2 + KZ_2 \cdot Y_{200}^2 \cdot (KCX_1 + KCX_2) \end{bmatrix} \begin{bmatrix} Z \\ j_X \end{bmatrix} = \begin{bmatrix} R_Z \\ MX \end{bmatrix} \tag{4.63}$$

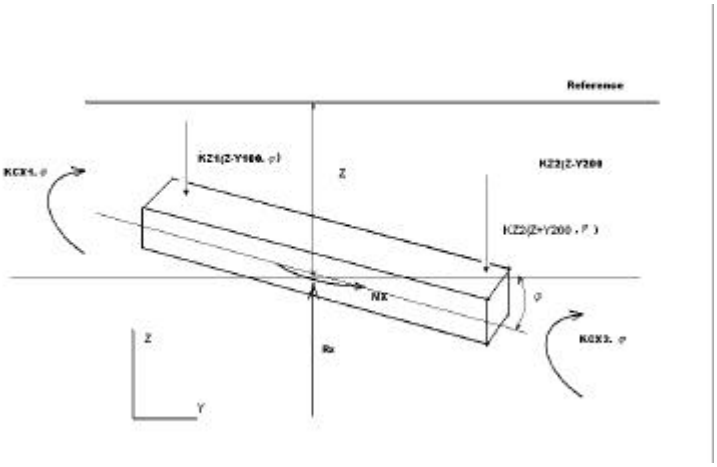

Figure 4.15. The spring forces and moments in z-direction.

The displacement and the angle rotation, which is shown in the figure 4.15, was calculated in the centre of the drum and by using virtual woke done method the displacements $Z_1$and Z_2 at the rubber elements can be calculated for the vibrated and drive side respectively:

$$Z_1 = Z - Y_{100} \cdot j_X \tag{4.64}$$

$$Z_2 = Z + Y_{200} \cdot j_X \tag{4.65}$$

The forces and moments can be calculated at the rubber elements

$$FZ_1 = KZ_1 \cdot Z_1 \tag{4.66}$$

$$FZ_2 = KZ_2 \cdot Z_2 \tag{4.67}$$

$$MX_1 = KCX_1 \cdot j_X \tag{4.68}$$

$$MX_2 = KCX_2 \cdot j_X \tag{4.69}$$

By the same previous assumptions the longitudinal spring forces can be calculated according to the free body diagram, which is shown in the figure 4.16.

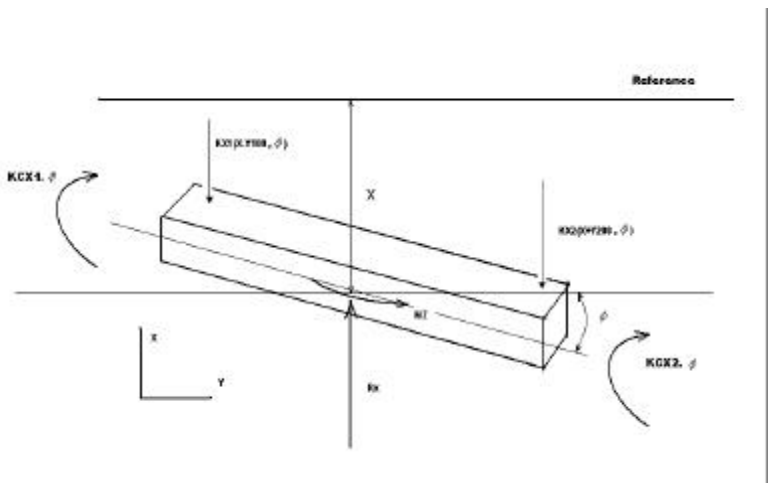

Figure 4.16. The spring forces and moments in x-direction

The equations of motion indicate static coupling

$$MD_1 \cdot \ddot{X} + (KX_1 + KX_2) \cdot X + (KX_2 \cdot Y_{200} - KX_1 \cdot Y_{100}) \cdot f_Z = FX \quad (4.70)$$

$$J\ddot{f} + (KX_2 \cdot Y_{200} - KX_1 \cdot Y_{100}) \cdot X + \left[KX_1 \cdot Y_{100}^2 + KX_2 \cdot Y_{200}^2 + KCZ_1 + KCZ_2\right] \cdot f_Z = MZ \quad (4.71)$$

Longitudinal braking or friction force

$$FX = \frac{FB_1}{2} + \frac{FB_1}{2} \quad (4.72)$$

Longitudinal acceleration

$$\ddot{X} = A_X \quad (4.73)$$

The resultant force in x-direction if the moment of inertia is zero

$$R_X = FX - MD_1 \cdot A_X \quad (4.74)$$

$$MZ = \frac{FB_2}{2} \cdot \frac{W_1}{2} - \frac{FB_2}{2} \cdot \frac{W_1}{2} \quad (4.75)$$

The matrix equation was

$$\begin{bmatrix} KX_1 + KX_2 & KX_2 \cdot Y_{200} - KX_1 \cdot Y_{100} \\ KX_2 \cdot Y_{200} - KX_1 \cdot Y_{100} & KX_1 \cdot Y_{100}^2 + KX_2 \cdot Y_{200}^2 + (KCZ_1 + KCZ_2) \end{bmatrix} \begin{bmatrix} X \\ f_Z \end{bmatrix} = \begin{bmatrix} R_X \\ MZ \end{bmatrix} \quad (4.76)$$

The displacement and the angle rotation were calculated in the centre of the drum and by using the previous virtual woke done method the displacements $X_1$and X_2 at the rubber elements can by calculated for the vibrated and drive side respectively:

$$X_1 = X - Y_{100} \cdot f_Z \quad (4.77)$$

$$X_2 = X + Y_{200} \cdot f_Z \quad (4.78)$$

The spring forces and the corresponding moments

$$FX_1 = KX_1 \cdot X_1 \tag{4.79}$$

$$FX_2 = KX_2 \cdot X_2 \tag{4.80}$$

$$MZ_1 = KCZ_1 \cdot f_Z \tag{4.81}$$

$$MZ_2 = KCZ_2 \cdot f_Z \tag{4.82}$$

In order to get the lateral forces and displacements the coordinates were changed and the same assumptions used but the stiffness matrix was diagonal and that mean static uncoupled equation was used to define the displacement and the rotational angle [8].

$$MD_1 \cdot \ddot{Y} + \left(KY_1 + KY_2\right) \cdot Y = FY \tag{4.83}$$

Where the external lateral force

$$FY = FYB_1 + FYB_2 \tag{4.84}$$

The lateral acceleration

$$\ddot{Y} = A_Y \tag{4.85}$$

At the centre of the drum

$$MX = \frac{FB_2}{2} \cdot \frac{W_1}{2} \cdot h_F - \frac{FB_2}{2} \cdot \frac{W_1}{2} h_F - FY \cdot R \tag{4.86}$$

Where R is the radius of the drum

The resultant force in y-direction if the moment of inertia is zero

$$R_y = FY - MD_1 \cdot A_Y \tag{4.87}$$

The matrix equation

$$\left(KY_1 + KY_2\right) \cdot Y = R_Y \tag{4.88}$$

This displacement is the same for the vibrated and drives side so that the forces and moment calculated

$$FY_1 = Y \cdot KY_1 \tag{4.89}$$

$$FY_2 = Y \cdot KY_2 \tag{4.90}$$

The same procedure and assumptions were used to calculate the spring forces and the moments for the rear drum.

4.4 Steering hitch

The Steering Hitch joins the front body with the rear one and it is consisted of:

- Steer joint hold (the bracket), which was attached with the back frame.
- Steer joint link, which was attached with front frame.
- Steer joint.
- Back steer link, which was attached with steer joint hold.
- Two hydraulic cylinders were placing at the Steering Hitch in order to allow the Asphalt Roller to turn left and right.

The x-axis is the steering axis and z-axis is the tilting axis. Figure 4-18 and 4-19 show the Steering Hitch and its available model.

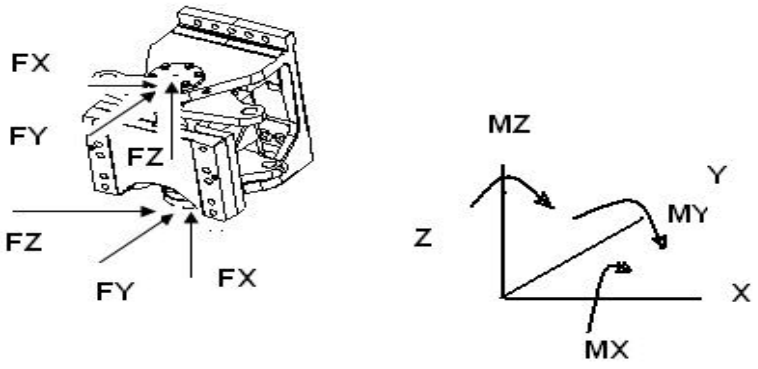

Figure 4.17. Steering hitch.

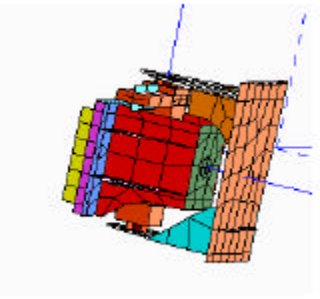

Figure 4.18. Available model.

The resultant forces at each coordinate were calculated and specified as internal load point 6 for the front view and internal load point 7 for the rear view.

4.5 Front and Rear mass of the Asphalt Roller

The Asphalt Roller was split into two parts in order to calculate the forces and moments at the Steering Hitch point. The front mass MF was consisted of a Water tank, Vibrated Fork; Drive Fork, Driver Seat and ROPS. The rear mass MR was consisted of an Oil tank, Vibrated fork, Engine, Water tank, Drive Fork and the Yoke. To realize the equilibrium conditions the forces and moments for the front mass at the Steering Hitch should be equal to the forces and moments for the rear mass but in the opposite direction. The location of the centre of gravity and all dimensions were taken from the available model which is shown in the figure 4.21 and 4.22 and the general equilibrium equations, which were governing the forces and moments according to the Newton's first and second law as below:

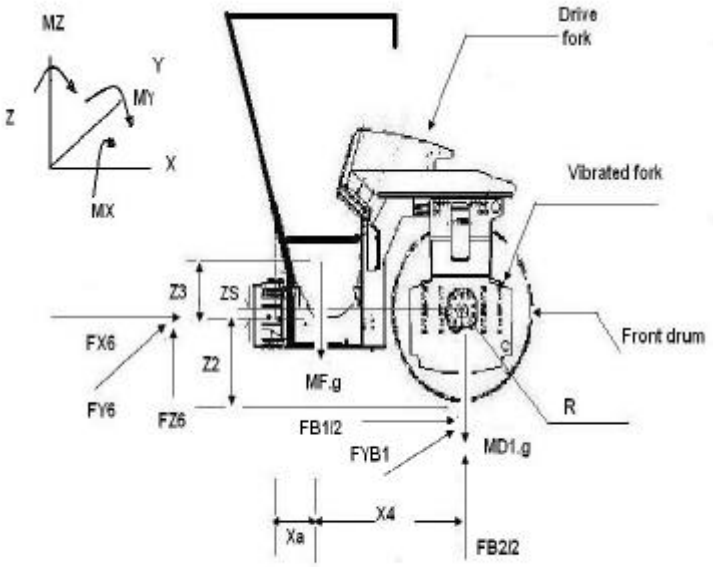

Figure 4.19. Front mass MF with the front drumMD_1.

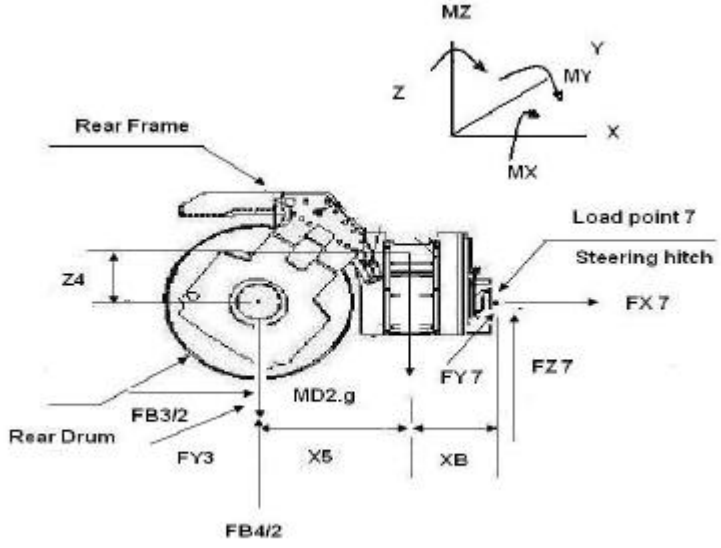

Figure 4.20. Rear mass with the rear drumMD_2.

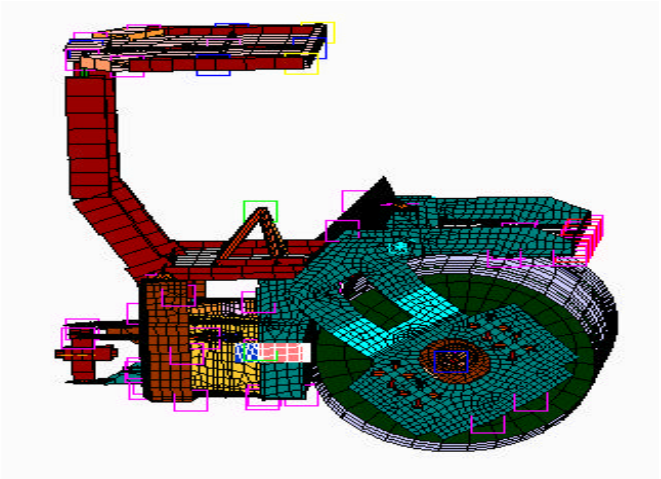

Figure 4.21. Available front mass of the roller MF and the front drum$MD_{1.}$

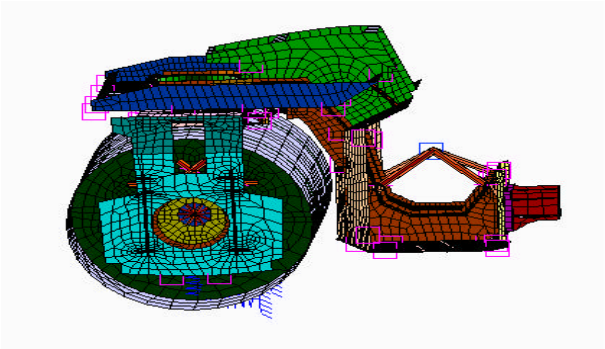

Figure 4.22. Available.rear mass with the rear drum$MD_{2.}$

From the free body diagrams which showed in the figure 4.19 and 4.20

$$\sum FZ = 0 \tag{4.91}$$

$$FZ_6 = (MF + MD_1) \cdot g \cdot \cos q - FB_2 \tag{4.92}$$

$$FZ_7 = FB_4 - (MR + MD_2) \cdot g \cdot \cos q \tag{4.93}$$

$$\sum FX = mass \cdot A_X \tag{4.94}$$

$$FX_6 = (MF + MD_1)\cdot A_X - FB_1 - (MF + MD_1)\cdot g \cdot \sin q \quad (4.95)$$

$$FX_7 = FB_3 + (MR + MD_2)\cdot g \cdot \sin q - (MR + MD_2)A_X \quad (4.96)$$

$$\sum FY = 0 \quad (4.97)$$

$$FY_6 = (MF + MD_1)\cdot A_Y - (FYB_1 + FYB_2) \quad (4.98)$$

$$FY_7 = (FYB_3 + FYB_4) - (MR + MD_2)\cdot A_Y \quad (4.99)$$

The moment at the centre of the drums

At the centre of drum

$$\sum MY = 0 \quad (4.100)$$

$$MY_6 = MF \cdot g \cdot X_4 \cdot \cos q - FZ_6 \cdot X_1 + MF[g \cdot \sin q - A_X](Z_3 - Z_S) + FX_6 \cdot Z_S + MY_2 \quad (4.101)$$

$$MY_7 = MR \cdot g \cdot X_5 \cdot \cos q + FZ_7 \cdot X_3 - MR[g \cdot \sin q + A_X](Z_4 - Z_S) - FX_7 \cdot Z_S + MY_{13} \quad (4.102)$$

$$\sum MZ = 0 \quad (4.103)$$

$$MZ_6 = MF \cdot A_Y \cdot X_4 - FY_6 \cdot X_1 \quad (4.104)$$

$$MZ_7 = MR \cdot A_Y \cdot X_5 + FY_7 \cdot X_3 \quad (4.105)$$

4.6 Front mass section MS

The front mass of the Asphalt Roller was cut by section A-A. The interested mass MS was consisted of the front Steering Hitch, Platform, Driver seat place and ROPs (Roll over protection structure). The forces and moments were calculated at load point 5, which was specified at the section A-A. This point was located at the same z-coordinate as the centre of gravity of the mass MS to decrease the number of equations. Figures 4.23 and 4.24 show the free body diagram of this rigid body

and the available corresponding rigid model, which was useful to get the dimensions.

$$\sum FX = mass \cdot A_X \tag{4.106}$$

$$FX_5 = MS \cdot A_X - MS \cdot g \cdot \sin q - FX_6 \tag{4.107}$$

$$\sum FZ = 0 \tag{4.108}$$

$$FZ_5 = MS \cdot g \cdot \cos q - FZ_6 \tag{4.109}$$

$$\sum FY = 0 \tag{4.110}$$

$$FY_5 = MS \cdot A_Y - FY_6 \tag{4.111}$$

At the internal load point 5

$$\sum MY = 0 \tag{4.112}$$

$$MY_5 = FZ_6 \cdot X_{100} - MS \cdot g \cdot \cos q \cdot X_{200} + MY_6 \tag{4.113}$$

$$\sum MZ = 0 \tag{4.114}$$

$$MZ_5 = MS \cdot A_Y \cdot X_{200} - FY_6 \cdot X_{100} - MZ_6 \tag{4.115}$$

The moment in x-axis didn't include in the calculations because the mass MS was located at y-axis.

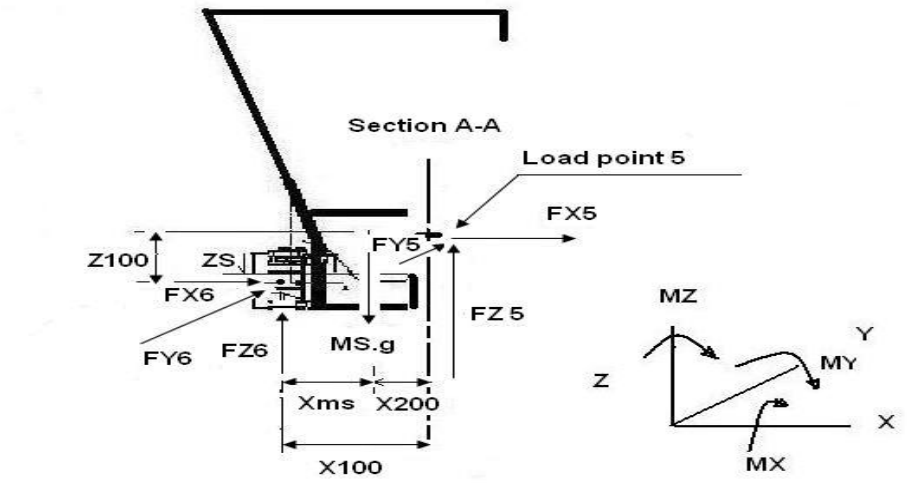

Figure 4.23. Front mass section MS.

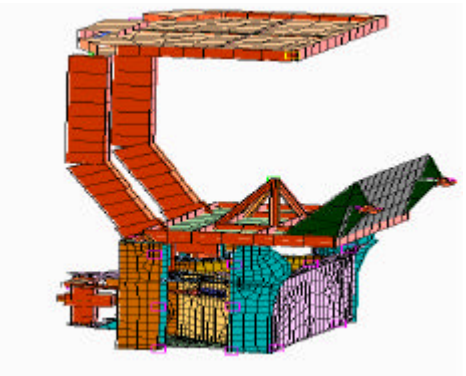

Figure 4.24. Available model of the front mass section Ms.

4.7 Rear mass section MK

Section B-B was taken on the rear part of the Asphalt Roller. Interested mass MK was studied. It consisted of rear Steering Hitch, Oil tank, the Engine and its supports, forces and moments were calculated at load point 8, which was located at the same z-coordinate as the centre of gravity of the mass MK for the same previous reason (4.6). Figures

4.25 and 4.26 were showed the free body diagram for this rigid body and the available corresponding model.

The general equations that applied for this rigid body were

$$\sum FX = mass \cdot A_X \tag{4.116}$$

$$FX_8 = MK \cdot A_X - MK \cdot g \cdot \sin q + FX_7 \tag{4.117}$$

$$\sum FZ = 0 \tag{4.118}$$

$$FZ_8 = MK \cdot g \cdot \cos q + FZ_7 \tag{4.119}$$

$$\sum FY = 0 \tag{4.120}$$

$$FY_8 = MK \cdot A_Y + FY_7 \tag{4.121}$$

At load point 8

$$\sum MY = 0 \tag{4.122}$$

$$MY_8 = FZ_7 \cdot X_{300} - MK \cdot g \cdot \cos q \cdot X_{400} + FX_7 \cdot Z_{200} + MY_7 \tag{4.123}$$

$$\sum MZ = 0 \tag{4.124}$$

$$MZ_8 = FY_7 \cdot X_{300} + MZ_7 - MK \cdot A_Y \cdot X_{400} \tag{4.125}$$

The moment in X-X axis didn't include in the calculations because then mass located at Y-axis.

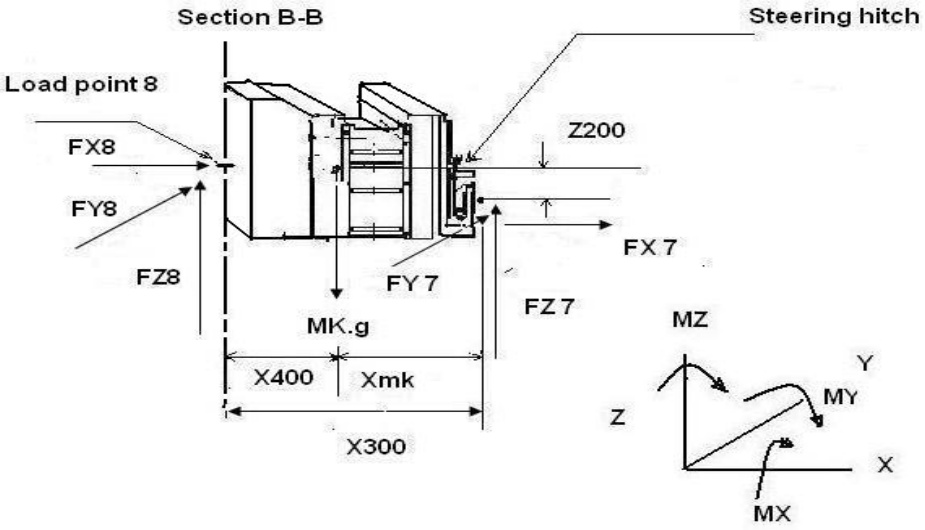

Figure4.25.Rear mass section MK.

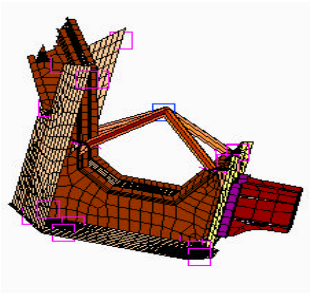

Figure4.26.Available model of the rear mass section MK.

4.8 Second rear mass section MH

The section C-C was used to cut at the Pivot bearing of the Yoke in the rear body to compute the forces and their corresponding moments at the internal load point 9. This was located at the same z-coordinate as the centre of gravity of the interested mass MH. It consisted of a Water tank and its supports. Available section mass MH that is shown in the figure 4.28 was useful to get the dimensions and the location of the centre of the gravity.

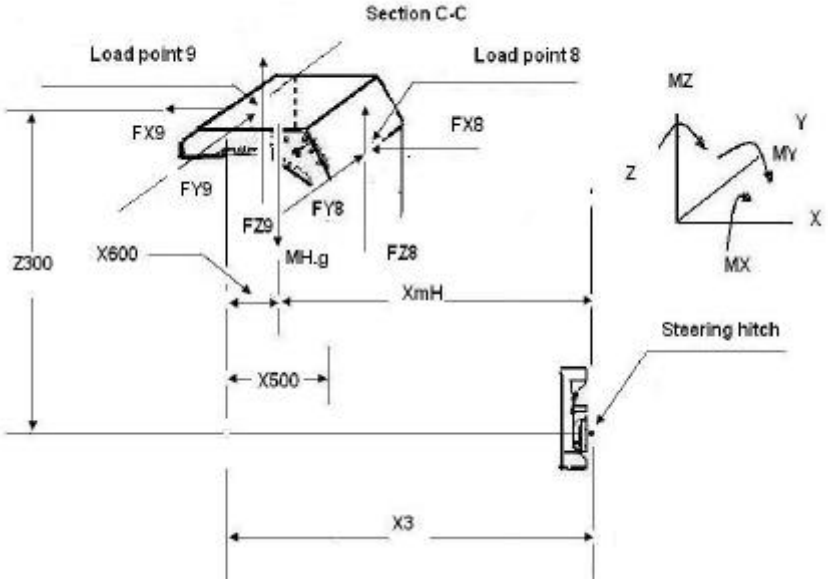

Figure 4.27 Rear mass section MH.

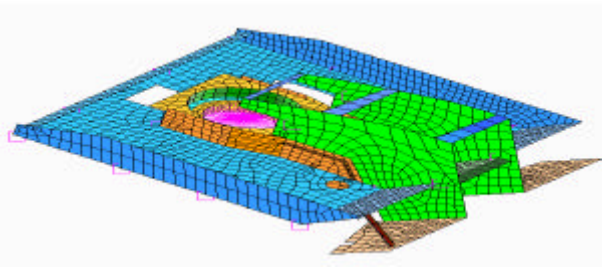

Figure4.28.Available model of the rear mass section MH.

General equations that governed this rigid body according to the free body diagram in the figure 4.27

$$\sum FX = mass \cdot A_X \tag{4.126}$$

$$FX_9 = MH \cdot A_X - MH \cdot g \cdot \sin q + FX_8 \tag{4.127}$$

$$\sum FZ = 0 \tag{4.128}$$

$$FZ_9 = MH \cdot g \cdot \cos q + FZ_8 \quad (4.129)$$

$$\sum FY = mass \cdot A_Y \quad (4.130)$$

$$FY_9 = MH \cdot A_Y + FY_8 \quad (4.131)$$

At load point 9

$$\sum MY = 0 \quad (4.132)$$

$$MY_9 = FZ_8 \cdot X_{500} - MH \cdot g \cdot \cos q \cdot X_{600} + FX_7 \cdot Z_{200} - MY_8 \quad (4.133)$$

$$\sum MZ = 0 \quad (4.134)$$

$$MZ_9 = MH \cdot A_Y \cdot X_{600} + FY_8 \cdot X_{500} - MZ_8 \quad (4.135$$

5 Simulation model

5.1 Modelling methods of an Asphalt Roller in I-DEAS®

The simulation model in I-DEAS is the simplifications of the physical vehicle .those simplifications limit the model's ability to produce the motion. A simple model might be describing the most important Asphalt Roller properties. I-DEAS® is one of the software suitable for building and simulating mechanical systems with movable parts after specifying as rigid bodies. I-DEAS® uses the Newton's second law

$$\sum \{F\} = m.\{a\}$$

Where F (N) is the force in 3D, m (Kg) is the mass and a (m/s^2) is the acceleration.

The geometry of the model was the nominal design of the Asphalt Roller, while the mass and stiffness properties were described by parameters. The main reason of building the model in I-DEAS® is to verify the theoretical model which was built in MATLAB® and to investigate the load equations and the directions of the element forces and their corresponding moments as well as to check the displacements of the Asphalt Roller and especially at the rubber elements for each load case.

The model contains 11 lumped masses, which are connected by joints as linear rectangular beams, rotational and translation springs were used to model the rubber elements on the vibrated and drive fork. Assumptions were carried on when building the model in I-DEAS:

- The rigid bodies in the simulation model were specified as eleven lumped masses.
- The Asphalt Roller was described with beam elements of a rectangular geometry $[100 \cdot 100mm]$. This kind of beam was used to join the lumped masses and other parts.
- All parts, except springs, were assumed rigid.

- Frictions in all joints were assumed negligible.
- The drum was modelled as a unsymmetrical rigid bar and beam elements were used to connect the drum centre, drum edges and elastic springs.
- The front and rear vibrated forks were released to apply torque about y-coordinate which was necessary for some cases.
- The rubber elements were modelled as torsion and translation springs according to the number and geometry of the rubbers.
- The external and internal load points specified as nodes in the model.
- High Young modulus was used to decrease the elasticity and increase the rigidity of the model especially for lifting case where four lifting loads were applied.
- The Steering Hitch was released for the steering load case under gravity in order to apply torque about z-axis.

The complete I-DEAS® model was used to deal with several cases by referring to the boundary conditions and the theoretical model. The location of the centre of the gravities, Internal and external forces were scaled from the Steering Hitch point, which considered as a reference. Different restraints were used to limit the motion of the Asphalt Roller according to the load case.

5.2 Drums model

The drum model was the most important components, which was difficult to describe in a simulation model, where both accurate results and quick computations are required. Structurally, the drum is a metal Shell with Bearings, Bearing Housings. Eccentric shaft and the drum Heads. All these components put as a single lumped mass (MD_1) on a rigid bar. Super linear translation and rotational springs with the values mentioned in (4.1) and (4.2) were used to describe the displacements of the rubbers in 3D. The drum is not symmetric where the drumhead from the vibrated side is larger than the drive side. The external reaction forces between the ground and the drum were acting on the bearings and then went to the rubber elements.

5.3 Gravity model

In this model no longitudinal friction forces were used and a gravitational force g in z coordinate applied from the boundary conditions. From the 'visualizer' in post processing icon the results of the element forces, moments and displacements for the load points were verified. The displacement restraints on the external nodes 1, 2, 9 and 10 were specified as below

- The rotation was free in x, y and z coordinates.
- The translation for the first external point was fixed in 3D.
- The translation for the second external point was fixed in x and z whiles it was free in y-axis.
- The translation for the ninth and tenth external points was fixed z-axis while it was free in x and y-axis.

Hence, the front drum had the ability to rotate in y-coordinate while the rear one rotated in x and y-axis.

5.4 Acceleration model

The same model was used but with different boundary conditions where a longitudinal deceleration with 0.5g (A_X) as a rectilinear motion applied to the left and the vibrated forks were released in order to get the torque about y-coordinate. Longitudinal friction forces between the drums and the ground were applied on the rear drum as input with value computed according to the (3.4). The same displacement restraints for the gravity were used on the external nodes. The steering hitch was locked.

5.5 Maximum torque model

This case was close to the gravity but the Asphalt Roller was operating under different and special boundary conditions when the drums are 'stuck and slip' in a clay road or something else. For this purpose the

drums would rotate with maximum torque, which was applied on the drums as input value according to (3.3) and a gravitational force 1g was used downward. Same restraints were specified. No friction forces or any other kind of quasi-static loads were considered namely no rectilinear motion was assumed.

5.6 Lifting model

The Asphalt Roller was modelled during the lifting operation so that no longitudinal and normal forces between the ground and drums were considered and the boundary conditions were changed by applying lifting forces at the eyelet points as input value, which mentioned in (3.5). Acceleration 1.6g in z-coordinate was applied upward. The Steering Hitch was locked during the lifting operation. The location of the front eyelet points was not equal to the rear one according to the theoretical model and the design of the Asphalt Roller itself. The displacement restraints were specified for the eyelet point 3, 4, 6 and 7 as:

- The rotation was free in x, y and z -coordinates.
- The translation for the third, fourth and sixth external point was fixed in x and z while it was free in y- axis.
- The translation for seventh external point was fixed in 3D.

5.7 Pulling model

A pulling force was applied as input value at the pulling eyelet node in x-direction to the left. Gravitational acceleration 1g in z-coordinate was applied downward. The Asphalt Roller was considered moving with constant velocity during the pulling operation and that means the longitudinal deceleration was zero and no rectilinear motion was occurred. Frictional forces were applied on the rear drum and in opposite side to the pulling force. The displacement restraints were specified to govern the motion as below:

- The rotation was free in x, y and z-coordinates.

- The translation for the first and second external point was fixed in 3D.
- The translation for the ninth and tenth external load was fixed in z and y-coordinate while it was free in x to display the motion during the pulling operation.

That means the motion of the Asphalt Roller was free in x-axis on the rear body while it was fixed on the front body to display the effect of pulling force at the rear part.

5.8 Towing model

A Towing force was applied at the towing eyelet node as input value in x-direction to the right. Gravitational acceleration 1g was applied downward while the longitudinal friction forces were applied on the rear drum in the opposite side to the towing force. Constant velocity assumed in the model during the towing operation. The same restraints for the pulling model were used.

5.9 Steering gravity model

In this model the Steering Hitch was released to apply maximum input torque in z-direction clockwise with value mentioned in (3.8). A new node was created close to the Steering Hitch point to apply that torque. Gravitational acceleration was applied downward with the same restraints of the pulling model.

5.10 Steering lateral acceleration model

To model this case the Steering Hitch should be locked. Gravitational acceleration 1g in z direction was applied downward. Lateral acceleration 0.143 g (A_y) was applied to describe the effect of the centrifugal force when the Asphalt Roller was moved on a curvilinear road. Constant speed was considered in the model. The restraints were applied to make the Asphalt Roller steer to the left according to that lateral acceleration.

- The rotation was free in x, y and z-coordinates for all external points.
- The translation for the first external point was fixed in z-axis.
- The translation for the second external point was fixed in the x, y and z axis.
- The translation for the ninth external point was fixed in y and z-axis.
- The translation for the tenth external point was fixed in z-axis.

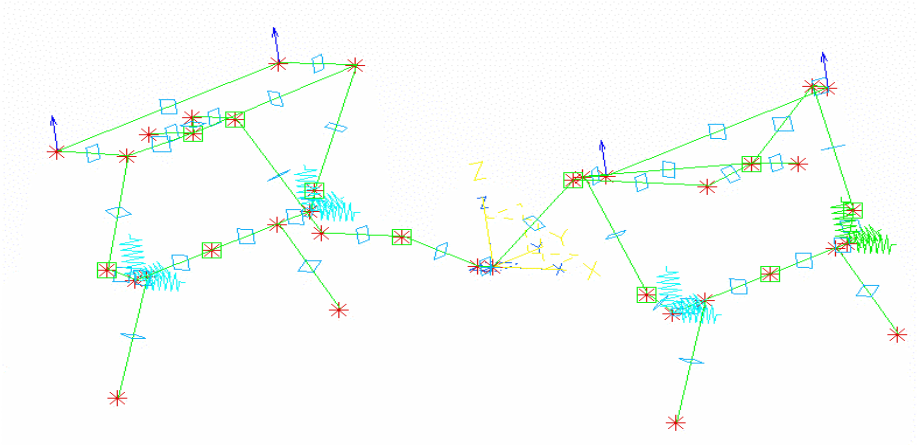

Figure 5.1. The lines of the model.

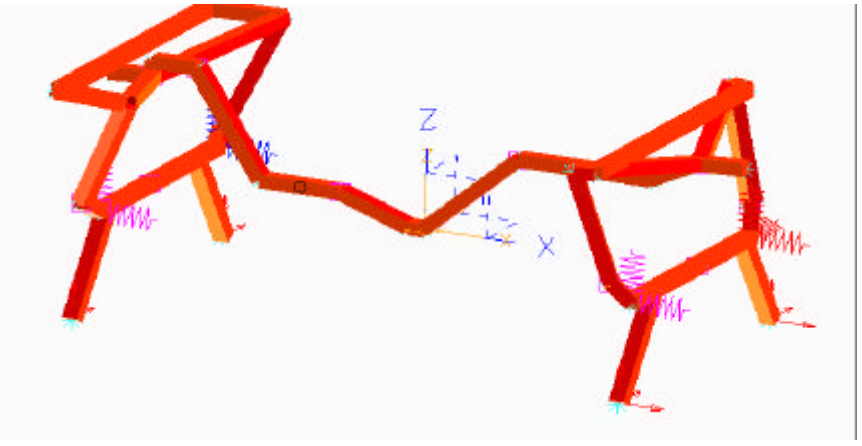

Figure 5.2 The general model of the Asphalt Roller as a shaded hardware in 3D

6 Results

The results for each load case were tabulated and plotted according to the two assumptions of the drums. The result of the theoretical model in MATLAB and the corresponding simulated model in I-DEAS are compared in tables. In the theoretical model the external forces assumed equal to at each edge of the drum but in I-DEAS simulation were not that and it shall be discussed later in the conclusion. The direction of the forces and moments were pointed from the rear to the front drum.

6.1 Gravity case

The internal element forces and corresponding moments by using the first assumption to calculate the forces of the rubber elements:

Table 6.1. Internal element force in MATLAB model.

Load point	FX	FY	FZ	MX	MY	MZ
1	0	0	-17243	0	0	0
2	0	0	-22004	0	0	0
3	0	0	-14840	2476	5268	0
4	0	0	-19406	7696	6839	0
5	0	0	-21070	0	7588	0
6	0	0	1248	0	25570	0
7	0	0	1248	0	25570	0
8	0	0	16885	0	15749	0
9	0	0	27490	0	-166	0
10	0	0	19076	-3117	6506	0
11	0	0	14250	-5781	4857	0
12	0	0	21336	0	0	0
13	0	0	16719	0	0	0

Table 6.2. Internal element forces in I-DEAS model.

Load point	FX	FY	FZ	MX	MY	MZ
1	0	1090	-17100	317	0.0241	27.6
2	0	-1090	-22100	1780	0.581	033.6
3	0	-1090	-14700	1070	5260	42.2
4	0	1090	-19500	8460	6830	31.5
5	0	0	-21000	0	7550	0
6	0	0	1290	0	25500	0
7	0	0	1290	0	25500	0
8	0	0	16900	0	15600	0
9	0	0	27500	0	-11	0
10	0	572	17800	-6020	6050	52.1
11	0	-572	15100	-5080	5190	11.1
12	0	-572	20100	-3660	0.0175	0
13	0	572	17600	-463	0.0175	0

This table shows the external load results for two models at the load point 1, 2, 9, and 10

Table 6.3 External forces.

Load point	Theoretical FZ	Simulation FZ
1	31980	32800
2	31980	31100
9	31516	32211
10	31516	30500

6.2 Maximum torque load case

The first assumption was used to calculate the rubber elements forces and make the comparison with I-DEAS model in order to verify the internal and external element forces with corresponding moments:

Table 6.4. External forces.

Load point	Theoretical FZ	Simulation FZ
1	27758	29200
2	27758	26300
9	35738	37000
10	35738	34100

Table 6.5. Internal element force in MATLAB model.

Load point	FX	FY	FZ	MX	MY	MZ
1	0	0	-13534	0	0	0
2	0	0	-17270	0	-15600	0
3	0	0	-11130	1891	-4018	0
4	0	0	-14672	5980	-20843	0
5	0	0	-12626	0	20436	0
6	0	0	9692	0	25583	0
7	0	0	9692	0	25583	0
8	0	0	25329	0	6414	0
9	0	0	35933	0	-15434	0
10	0	0	23810	-3864	-8116	0
11	0	0	17960	-7126	9481	0
12	0	0	26070	0	15600	0
13	0	0	20429	0	0	0

Table 6.6. Internal element force in I-DEAS model.

Load point	FX	FY	FZ	MX	MY	MZ
1	0	0	-14200	287	0	0
2	0	0	-16600	1770	-15600	0
3	0	0	-11800	-999	-4700	0
4	0	0	-14000	-6810	-20100	0
5	0	0	-12600	0	20400	0
6	0	0	9730	0	25500	0
7	0	0	9730	0	25500	0
8	0	0	25400	0	6260	0
9	0	0	36000	0	-15600	0
10	0	0	22600	-6970	-7180	0
11	0	0	18800	-6020	8680	0
12	0	0	25000	4160	0	0
13	0	0	21200	524	15600	0

Some differences at the moment in x-direction of the forks and the normal drum forces were occurred because the external normal load at each edge of the drum is creating a resultant moment in x-direction at the centre of the drum with value 3107 N.m according to I-DAES model while these external loads were assumed equal to each other in the theoretical model.

6.3 Acceleration load case

External loads tabulated below

Table 6.7. Normal external forces.

Load point	Theoretical FZ	Simulation FZ
1	22898	25100
2	22898	20900
9	40597	42400
10	40597	38200

Table 6.8. Longitudinal external forces.

Load point	Theoretical FX	Simulation FX
1	11449	11200
2	11449	11200
9	20299	20486
10	20299	20486

It can be noticed as before that the normal forces are equal to each other in the theoretical model but they are not that in I-DEAS which it will discuss later in chapter 7.these differences effect on the internal element forces of the forks and drums because the resultant moment in x-direction at the centre of the drum is equal to 4500 Nm in I-DEAS model but it did not considered in MATLAB®. The first assumption was used to verify the internal loads:

Table 6.9. Internal element force in MATLAB model.

Load point	FX	FY	FZ	MX	MY	MZ
1	4632	0	-9263	0	0	0
2	5910	0	-11821	0	16028	0
3	3430	0	-6860	1219	6097	0
4	4611	0	-9222	4005	24132	0
5	1453	0	-2906	0	24375	0
6	-9706	0	19411	0	20911	0
7	-9706	0	19411	0	20911	0
8	-17524	0	35048	0	10797	0
9	-22826	0	45653	0	53404	0
10	-14630	0	29260	-4722	-4566	0
11	-11115	0	22230	-8674	31962	0
12	-15759	0	31519	0	0	0
13	-12350	0	24700	0	28418	0

The longitudinal and normal forces were calculated while there was no effect for the moment in z-axis or any lateral force.

Table 6.10. Internal element force in I-DEAS model.

Load point	FX	FY	FZ	MX	MY	MZ
1	4530	167	-10800	268	0	7
2	5430	-167	-10500	1810	-16200	367
3	3320	-167	-8350	1020	6530	538
4	4130	167	-7880	5170	23400	1510
5	871	0	-3050	0	23900	9.7
6	-10300	0	19300	0	21000	9.7
7	-10300	0	19300	0	21000	9.7
8	-18100	0	34900	0	-10700	9.7
9	-23400	0	45500	0	53600	9.7
10	-15300	1950	28100	-7460	-5630	350
11	-10800	-1950	22900	-6390	-32500	400
12	-16400	-1950	30300	4840	0	300
13	-12100	1950	25300	598	-29400	9

6.4 Lifting load case

The external forces at the lifting eyelets were calculated. There existed no contact between the ground and the drums because the model was assumed the lifting operation. The internal forces and moments were more accurate than other cases. The second assumption was used in these tables where the moments of the drums could be calculated

Table 6.11. Internal element force in MATLAB model.

Load point	FX	FY	FZ	MX	MY	MZ
1	0	0	15779	188	0	0
2	0	0	23759	-2502	0	0
3	0	0	19625	-2682	-6187	0
4	0	0	27917	-11563	-8930	0
5	0	0	-43885	0	-8439	0
6	0	0	-8176	0	35795	0
7	0	0	-8176	0	35795	0
8	0	0	16843	0	31342	0
9	0	0	33811	0	13958	0
10	0	0	-19563	-2710	-6619	0
11	0	0	-27964	-11682	-9488	0
12	0	0	-15948	190	0	0
13	0	0	-24014	2529	0	0

No longitudinal and lateral element forces were occurred because accurate restraints were used at the lifting eyelets with high young modulus. The moment in x-direction could be calculated because of using the second assumption to calculate the rubber element forces and their torsion moments.

Table 6.12. Internal element force in I-DEAS model.

Load point	FX	FY	FZ	MX	MY	MZ
1	0	0	15800	188	0	0
2	0	0	23800	-2500	0	0
3	0	0	19600	-2680	-6190	0
4	0	0	27900	-11600	-8930	0
5	0	0	-43800	0	-8500	0
6	0	0	-8080	0	35600	0
7	0	0	-8080	0	35600	0
8	0	0	16900	0	31000	0
9	0	0	33900	0	13600	0
10	0	0	-19600	-2710	-6620	0
11	0	0	-28000	-11700	-9490	0
12	0	0	-15900	190	0	0
13	0	0	-24000	2530	0	0

It can be noticed that the compared results were more accurate because there was no contact between the ground and the drums which means there was no resultant moment in x-direction acting at the centre of the drums.

6.5 Pulling load case

The longitudinal and normal external load points comparison are shown in the table below

Table 6.13. Braking external forces.

Load point	Theoretical FX	Simulation FX
1	15009	15000
2	15009	15000
9	23652	23653
10	23652	23653

Table 6.14. Reaction external forces

Load point	Theoretical FZ	Simulation FZ
1	16191	19100
2	16191	13200
9	47305	50100
10	47305	44200

The same previous difference can be noticed here and because of that the resultant moment in the centre of the drum is equal to 6321 Nm in I-DEAS, which have been considered zero in MATLAB. Those differences were affected the internal drum and forks forces. The internal force sand corresponding moments were tabulated by using the first assumption:

Table 6.15. Internal element force in MATLAB model.

Load point	FX	FY	FZ	MX	MY	MZ
1	13189	0	-3370	0	0	0
2	16830	0	-4300	0	-21013	0
3	13189	0	-966	290	-13979	0
4	16830	0	-1710	1279	-38967	0
5	30018	0	-10508	0	-36978	0
6	30018	0	32826	0	12100	0
7	30018	0	32826	0	12100	0
8	30018	0	48463	0	51373	0
9	30018	0	59086	0	67182	0
10	-26521	0	37097	-5956	-14286	0
11	-20783	0	28072	-10805	-44651	0
12	-26521	0	39356	0	0	0
13	-20783	0	30542	0	-33113	0

No lateral force was calculated in that case and no moment in z-axis was noticed because the friction forces applied equally and in a same direction at each edge of the drum with resultant of moment zero.

Table 6.16. Internal element force in I-DEAS model.

Load point	FX	FY	FZ	MX	MY	MZ
1	12800	0	-1930	0	0	0
2	17200	0	-5700	0	-21800	0
3	12800	0	-669	2476	-13900	0
4	17200	0	-3290	7696	-38700	0
5	30000	0	-10500	0	-36900	0
6	30000	0	32900	0	12200	0
7	30000	0	32900	0	12200	0
8	30000	0	48500	0	51500	0
9	30000	0	59100	0	67400	0
10	-26800	0	36200	-3117	-14000	0
11	-20500	0	28400	-5781	-44500	0
12	-26800	0	38400	0	0	0
13	-20500	0	30800	0	-34000	0

Some differences were occurred because of the same previous reason

6.6 Towing load case

The external distribution forces by using the first assumption

Table 6.17. Braking external forces.

Load point	Theoretical FX	Simulation FX
1	-47612	-47600
2	-47612	-47600
9	-47612	-47621
10	-47612	-47621

Table 6.18. Reaction external forces

Load point	Theoretical FZ	Simulation FZ
1	70876	66200
2	70876	75500
9	-7381	-12300
10	-7381	-2870

It can be noticed that the same previous differences were occurred, especially at the rear drum where a large value considered at load point 10 successive of small negative value at point 9 while it was considered equal in MATALB but the resultant of these forces was the same. Differences in FZ create moment in x-direction at the centre of the front and rear drum with value 6750 N.m and 10000 N.m.

Table 6.19. Internal element force in MATLAB model.

Load point	FX	FY	FZ	MX	MY	MZ
1	40764	0	-46709	0	0	0
2	54477	0	-70330	0	-66670	0
3	40764	0	-44306	0	-24564	0
4	54477	0	-67731	0	-99683	0
5	-95243	0	-98826	0	-128583	0
6	-95243	0	-76545	0	52836	0
7	-95243	0	-76545	0	52836	0
8	-95243	0	-60907	0	40926	0
9	-95243	0	-50303	0	156688	0
10	-53398	0	-24538	0	-44194	0
11	-41845	0	-19928	0	-101061	0
12	-53398	0	-22279	0	0	0
13	-41845	0	-17459	0	-66670	0

No lateral force in y-axis or any moment in z-direction was calculated in this case because there was just an effect of the longitudinal pulling forces and the friction forces applied equally in the same x-direction which they were given zero resultant moment in z-axiz.

Table 6.20. Internal element force in I-DEAS model.

Load point	FX	FY	FZ	MX	MY	MZ
1	40400	8620	-43700	0	0	0
2	54800	-8620	-73300	0	-69200	0
3	40400	0	-41300	0	-25300	0
4	54800	0	-70700	0	-98500	0
5	-95200	0	-98800	0	-129000	0
6	-95200	0	-76500	0	52900	0
7	-95200	0	-76500	0	52900	0
8	-95200	0	-60900	0	40800	0
9	-95200	0	-50300	0	157000	0
10	-53900	0	-26900	0	-43900	0
11	-41400	0	-18000	0	-103000	0
12	-53900	-3570	-24600	0	0	0
13	-41400	3570	-15500	0	-68400	0

Some differences were occurred because of the unsymmetrical distribution of the external reaction forces.

6.7 Steering loads under gravity (model C)

The external loads are tabulated below

Table 6.21. Braking external forces.

Load point	THEORETICAL FX	SIMULATION FX
1	18665	17600
2	-18665	-17600
9	18665	19600
10	-18665	-19600

Table 6.22. Reaction external forces.

Load point	THEORETICAL FZ	SIMULATION FZ
1	31980	34100
2	31980	29800
9	31516	33400
10	31516	29200

Unsymmetrical distribution of the reaction forces was noticed between two models.

Table 6.23. Internal element force in MATLAB model.

Load point	FX	FY	FZ	MX	MY	MZ
1	12100	0	-15663	-186	0	7909
2	-12100	0	-23584	-2484	0	11642
3	-12100	0	-13260	2413	-16538	6003
4	12100	0	-20986	10753	-4432	7255
5	0	0	-21070	0	7588	40000
6	0	0	1248	0	25570	40000
7	0	0	1248	0	25570	40000
8	0	0	16885	0	15749	-40000
9	0	0	27490	0	166	-40000
10	-12100	0	17745	-8073	5847	-9736
11	12100	0	15581	-5890	17211	-3522
12	12100	0	20004	-5164	0	-11642
13	-12100	0	18050	387	0	-7909

Opposite longitudinal friction forces were created moment in z-direction. Input torque in z-axis with value 40000 N.m. was applied at the Steering Hitch. The second assumption was used in the tables to verify this case.

Table 6.24. Internal element force in I-DEAS model

Load point	FX	FY	FZ	MX	MY	MZ
1	11400	0	-16900	-285	0	7480
2	-11400	0	-22300	-3800	0	11800
3	-11400	0	-14500	2520	-16400	5800
4	11400	0	-19700	10800	-4260	7120
5	0	0	-21000	0	7550	38200
6	0	0	1290	0	25500	40000
7	0	0	1290	0	25500	40000
8	0	0	16960	0	15600	-41100
9	0	0	27500	0	11	-42000
10	-12700	0	17800	-7620	6030	-9960
11	12700	0	15200	-5050	17300	-3570
12	12700	0	20000	-3800	0	-12200
13	-12700	0	17600	285	0	-8290

Some difference of the moment in x-direction at the forks and the drum forces were occurred because of the same previous reason where the resultant moment in x-direction at the front and rear drum centre is 4607 and 4500 Nm respectively while it did not consider in MATLAB model.

6.8 Lateral acceleration case

The external loads in MATLAB and I–DEAS model were tabulated below:

Table 6.25 .Lateral external forces

Load point	Theoretical FY	Simulation FY
1	4561	4590
2	4561	4590
9	4561	4500
10	4561	4500

Table 6.26. Reaction external forces

Load point	Theoretical FZ	Simulation FZ
1	36063	38200
2	27432	25700
9	27432	28700
10	36063	34000

Unsymmetrical distribution was used in the theoretical model because the effect of the lateral acceleration .second assumption used to verify this case

Table 6.27. Internal element force in MATLAB model.

Load point	FX	FY	FZ	MX	MY	MZ
1	0	-1857	-18409	-559	0	0
2	0	-3714	-20839	-7466	0	0
3	0	-1512	-16005	3624	5661	-548
4	0	-3341	-18241	10810	6446	1335
5	0	-2960	-21070	0	-7588	-1315
6	0	246	1248	0	25570	3796
7	0	246	1248	0	25570	3796
8	0	2492	16885	0	15749	2312
9	0	4016	27490	0	166	-24
10	0	3364	18014	-6904	-6145	-1147
11	0	1490	15312	-7729	-5219	-508
12	0	3689	20273	7304	0	0
13	0	1845	17782	547	0	0

Constant speed was considered so that there was no effect for any longitudinal forces and lateral friction forces were appeared instead.

Table 6.28. Internal element force in I-DEAS model.

Load point	FX	FY	FZ	MX	MY	MZ
1	0	-1870	-18100	-364	0	0
2	0	-3760	-21100	-7850	0	0
3	0	-1530	-15700	3790	5660	-554
4	0	-3380	-18500	10600	6530	1180
5	0	-3020	-21000	0	-7550	-1080
6	0	185	1290	0	25500	3660
7	0	185	1290	0	25500	3660
8	0	2430	16900	0	15600	2240
9	0	3950	27500	0	11	-15
10	0	3280	17800	-6702	-6080	-1147
11	0	1450	15100	-7510	-5160	-495
12	0	3610	20100	7140	0	0
13	0	1800	17600	364	0	0

The values seem more accurate in this case because of that unsymmetrical distribution which was used in the theoretical model.

7 Conclusion

DYNAPAC compaction AB are developing several types of Roller, the assignment that is presented in this report has the aim to investigate the static and quasi-static loads of the Asphalt Roller for several load cases which are in consideration during the design. The theoretical model in MATLAB dealt with equilibrium equations and the equation of motion. The chosen investigation method was a mechanical system simulation with the software I-DEAS. The mechanical parts in the machinery were simulated as rigid bodies. The exception was to verify and identify all high forces and heavy bending moments in 3-D that might be of interest and to identify the weak and tough parts in the Roller through the force and moment diagrams for each of the load cases, something that might be fatal for the machinery. The agreement between the theoretical model in MATLAB® and the simulated one in I-DEAS® was quite accurate for the majority of the load cases. There was some disagreement in the forces of the drums and forks which can be notice in chapter 6. That happened because the external normal and longitudinal forces acting at the contact point between the drums and ground were assumed equally to each other in the theoretical MATLAB model but the simulation model in I_DESAS was not able to distribute these forces equally. This could be accounted to the un-symmetry in masses of the forks and the difference between the physical properties of the stiffness for the vibrated and drive side. The ‘main sections’ and the Steering Hitch had the results more accurate; this is because the equations dealt with the external resultant reaction forces without considering about the amount of the force at each edge of the drum. It was difficult to apply the first assumption, which used the equilibrium equation method to calculate the forces at the rubber elements for the Steering load under gravity (model C) because there was large moment in z-direction was applied at the Steering Hitch. One-half of this moment in z-axis is realized at the each side of the drum (at the rubber elements) and the remainder was observed due to the longitudinal internal forces acting on the rubber elements. The first assumption was not accurate to calculate the moments on the rubbers because these were torsion moments, which were dependent on the stiffness only. This affected the values of the moments on the forks. Small difference of the moment in z-direction was appeared at the Steering Hitch for the gravity steering case model A and B because that might be refer to

unequal friction forces that were used on the front and rear drum. One interesting result of these investigations that have been carried out showed that there was no abnormal force or moment was occurred for any of the load case.

In the future, a deeper investigation with the same basic theories, assumptions and methods that were used in this assignment can be performed.

8 Program Algorithm

The Algorithm showed the procedure which was used to deal with the theoretical model in MATLAB® where several load cases were specified as functions and all equations which has belonged the load case were implemented. These functions were combined with the main code. The main code was contained all load cases and the matrices which were calculating the external loads. Input data was written as a function in the program and it was loaded to the main script .The out text function was created to arrange the results, the date of work, constant values, and the definitions etc .in one out put text as table which was easier to read. The codes were created according to the properties and the free body diagrams of the Asphalt Roller.

The structure of the program is illustrated below

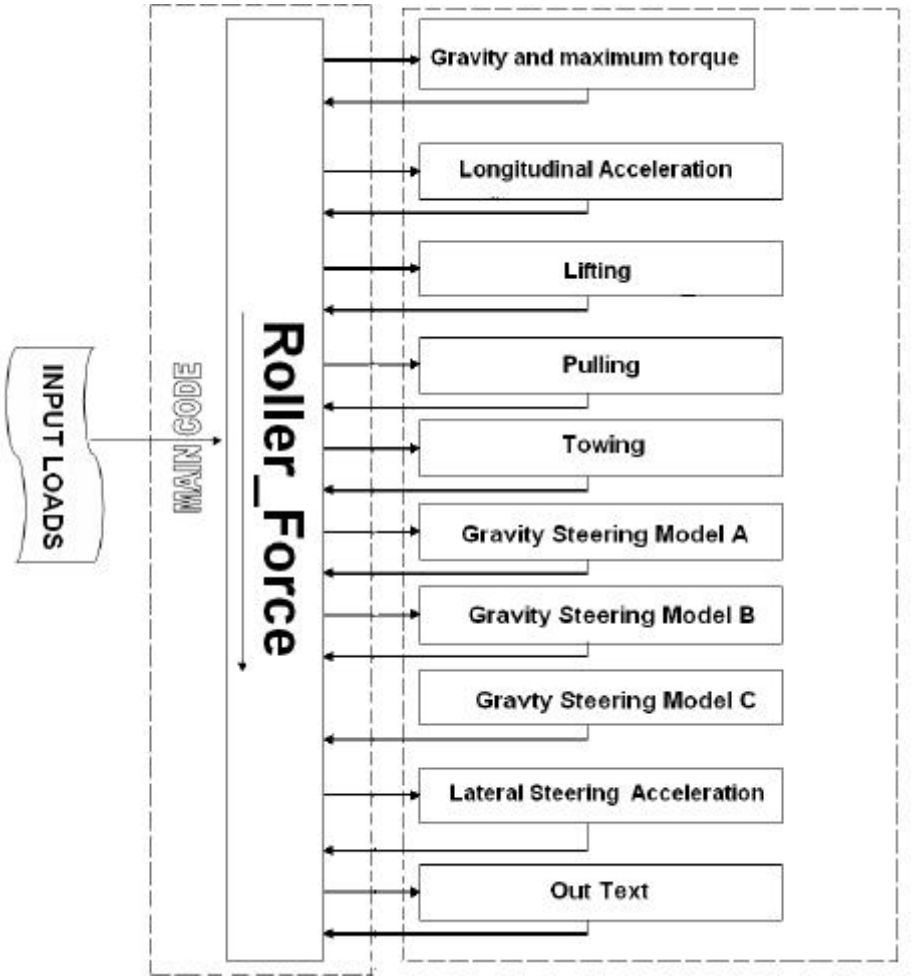

The main program was called Roller_Force and uses ten functions which include all load cases .The first function (INPUT LOADS) contains all specific data regarding the Asphalt Roller e.g. the different masses, the properties of the rubber elements and the locations of the centre of gravities. The function (Gravity and maximum torque) determines all forces and moments according to this load case. This function combines two load cases, which are the gravity, and maximum torque. The function (Longitudinal acceleration) determines forces and moments for all load points according to the model and the boundary conditions. The function (Lifting) presents the calculations during the lifting operation. Important forces and moments are determined according to the boundary conditions. The function (Pulling)

determines the forces and the moments during the pulling operation. The function (Towing) determines the forces and moments during towing operation for all load points. The function (Gravity steering model A) determines the forces and moments according to the first model (distributed external loads on the drum). Specific equations are used to find out the forces and moments at the drums. The function (Gravity steering model B) determines all forces and moments according to the second model (drum stands on a concave surface). The function (Gravity steering model C) determines all forces and moments according to the third model (maximum torque in z-axis as input). This model was verified in I-DEAS to check the forces and moments in 3D. The function (Lateral acceleration steer) determines the element forces and moments according to the lateral acceleration model in 3D. The function (Out text) displays all input data and all external and internal forces and moments as tables (texts) with comments for all load cases. Building the theoretical model was necessary and useful for the work because it can be used in future for several types of tandem rollers by changing the data in INPUT LOADS function without referring to I-DEAS simulation model.

9 References

1. ´´*Compaction And Paving(Theory And Practice)*´´,Svedala DYNAPAC,Publication no.1HCCCDAPEN1,Svedala AB.2000.
2. Meriam.J.L., Kraige .L.G.,´´*Engineering Mechanics, Static, Fourth Edition*´´, University of California and Virginia polytechnic institute and state university.1997.
3. Kraige.L.G, ´´*Engineering Mechanics, Dynamics, Fourth edition*´´, University of California (Santa Barbara) and Virginia polytechnic institute and state university.1997.
4. Lycken.T., ''*Lastfall Vid Dimensionering Av Vibrerande Vältar*'', Internal DYNAPAC report TR04063, DYNAPAC AB, Karlskrona, Sweden.2004.
5. Bång.L.K,´´*Lastning Och Säkring Av Gods I Lastbärare*´´, Sweden, Stockholm.1990.
6. Gillespie.D.T,´´*Fundamentals Of Vehicle Dynamics*´´,Society of automotive engineers,Inc.USA.1992
7. .Ramamrutham.S, ´´*A Text Book Of Applied Mechanics*´´, Sri Ram College of engineering, New Delhi.1994.
8. Thomason T.W., ´´*Theory Of Vibration With Application*´´, University of California, Santa Barbara.1992.
9. JR. W.W., Timoshenko.S.P, and, Young.D.H., ´´*Vibration Problems In Engineering, Fifth addition*´´, Stanford University.1998.

10 Appendices

Appendix A

This appendix shows the plots of the forces and moments by the comparison between MATLAB MODEL and I-DEAS model as well as the distribution of these forces and moments in 3D in the Gravity case

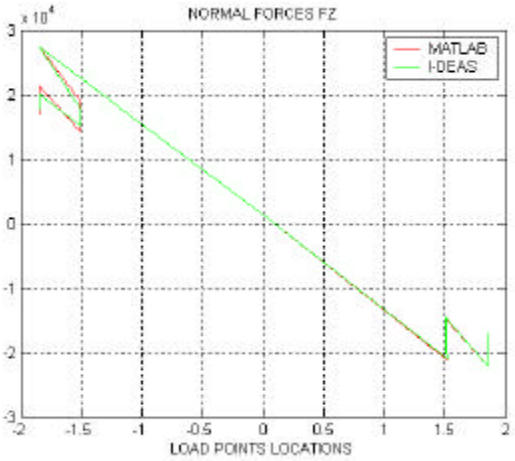

PoltA.1 Normal force in z-axis (Gravity case).

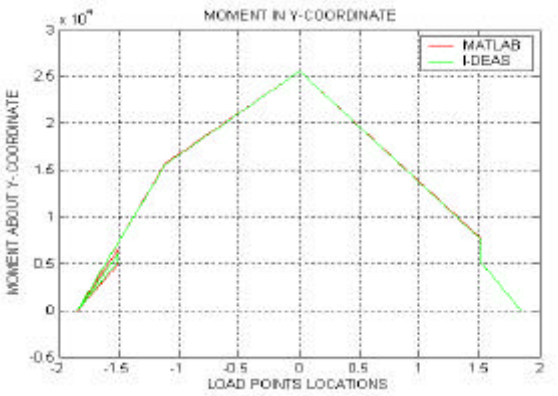

PlotA.2 Moment about y-axis (Gravity case).

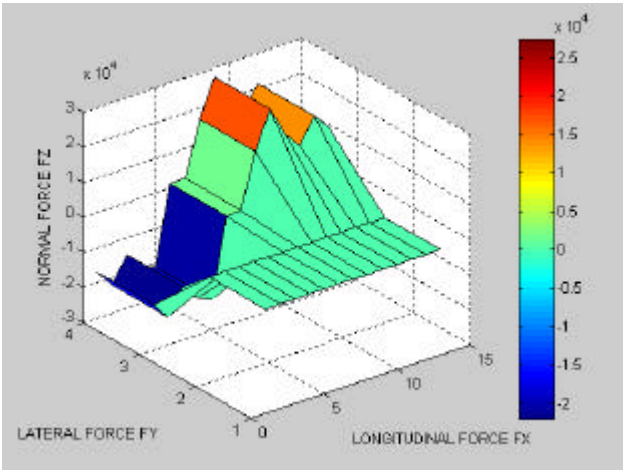

PlotA.3 Force distribution in 3D (Gravity case).

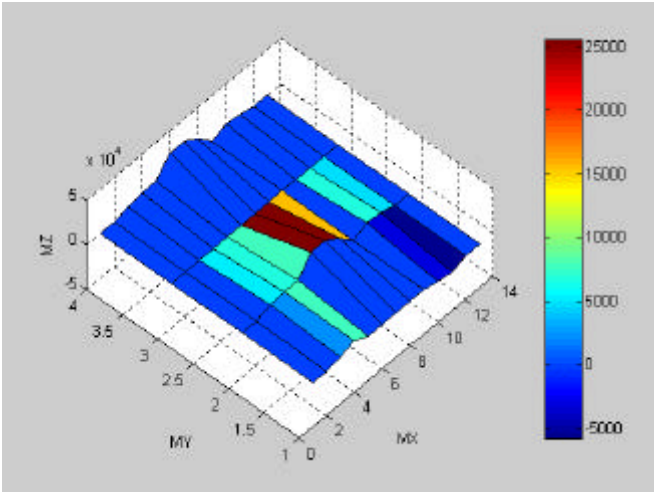

PlotA.4 Moment distribution about y-axis (Gravity case).

Appendix B

This appendix shows the plots of the forces and moments by the comparison between MATLAB MODEL and I-DEAS model as well as the distribution of these forces and moments in 3D in the Maximum torque case

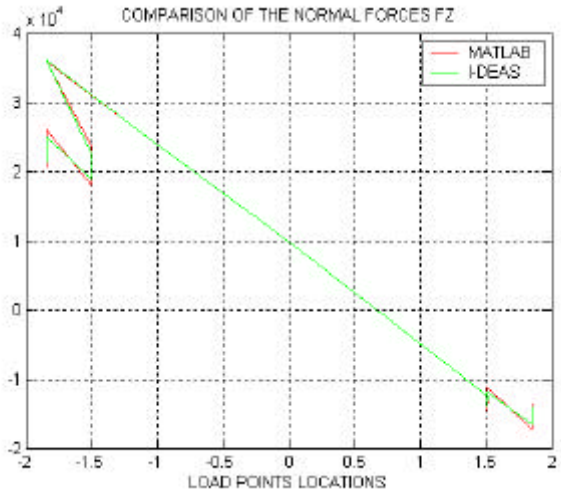

PlotB.1 Normal comparison force FZ.

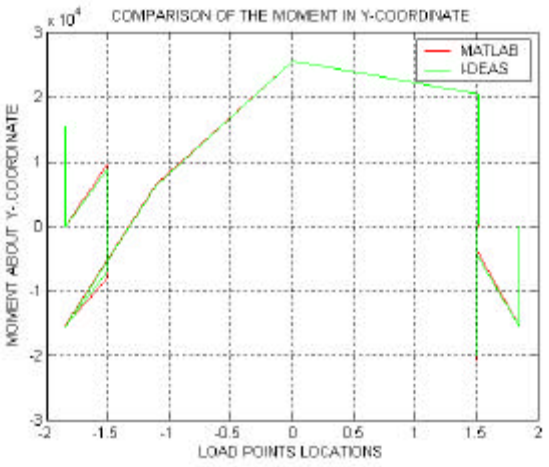

PlotB.2 Moment comparison about y-axis MY.

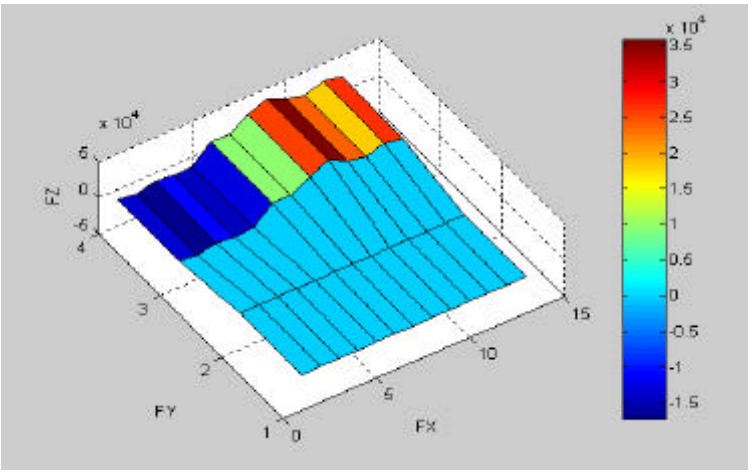

PlotB.3 Normal forces distribution in 3D.

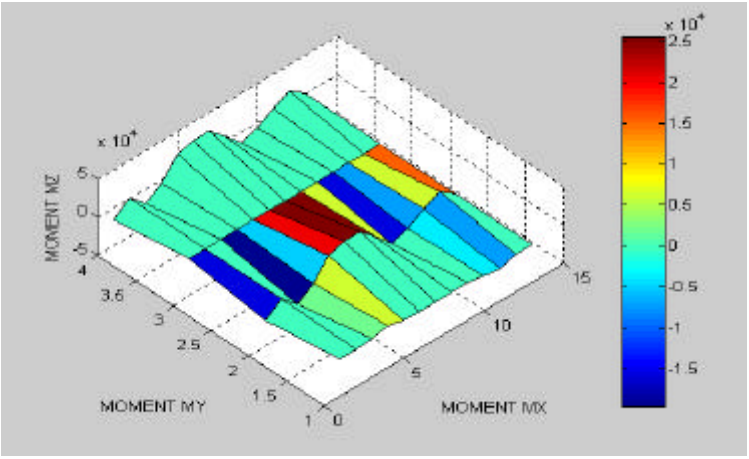

PlotB.4 Moment's distribution about y-axis.

Appendix C

This appendix shows the plots of the forces and moments by the comparison between MATLAB and I-DEAS model as well as the distribution of these forces and moments in 3D in the acceleration case.

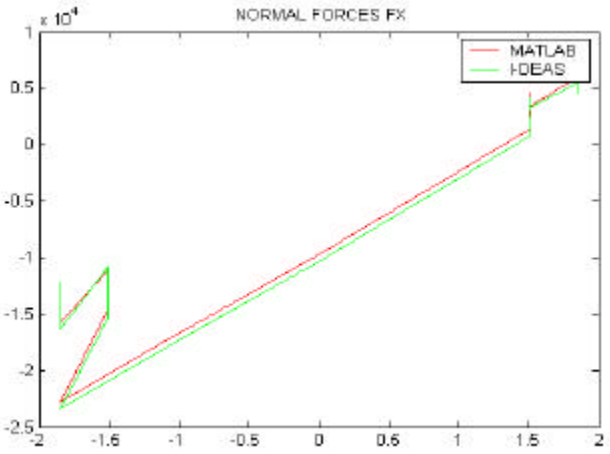

PlotC.1 Longitudinal force comparison.

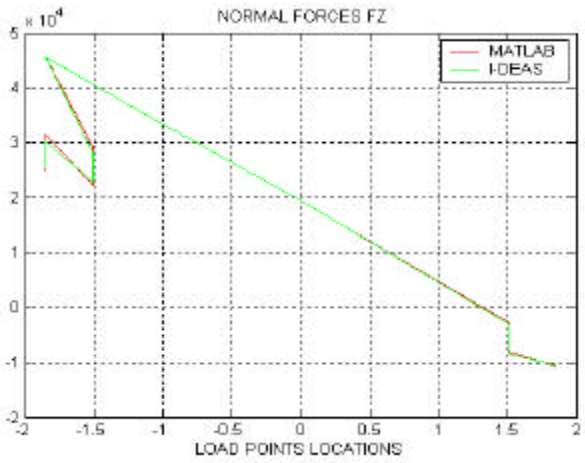

PlotC.2 Normal force comparison.

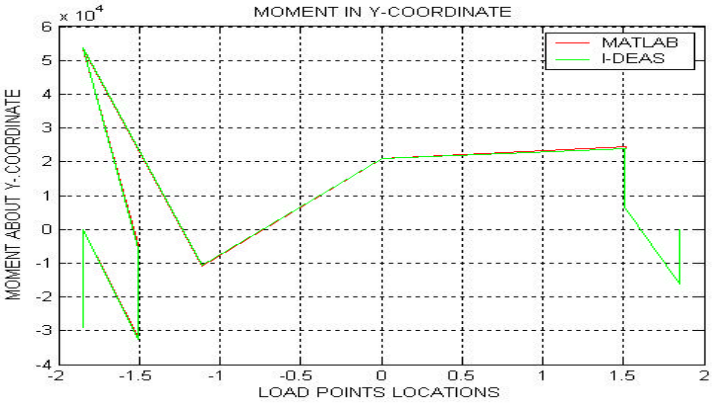

PlotC.3 Moment about Y-axis comparison.

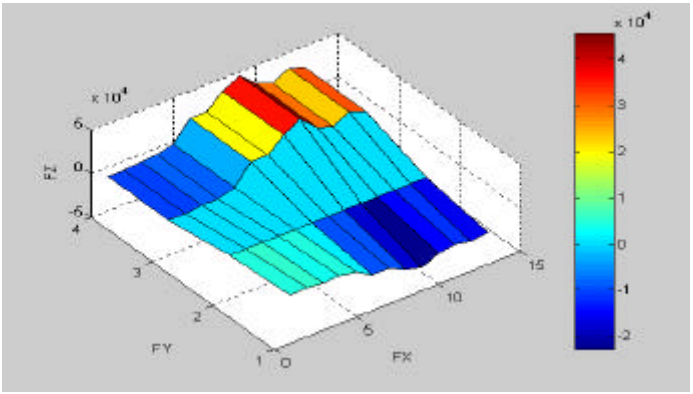

PlotC.4 Distribution of the forces in 3D.

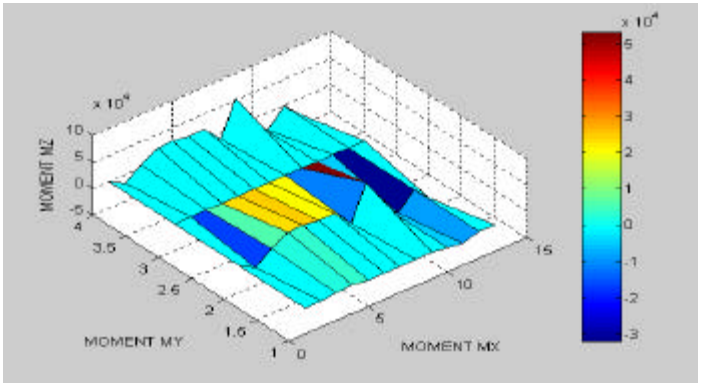

PlotC.5 Distribution of the moments in 3D.

Appendix D

This appendix shows the plots of forces and moments of the lifting load case

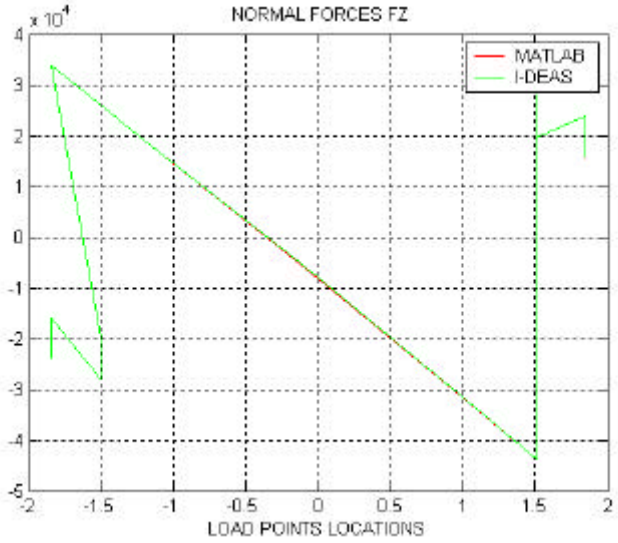

PlotD.1 Normal force comparison.

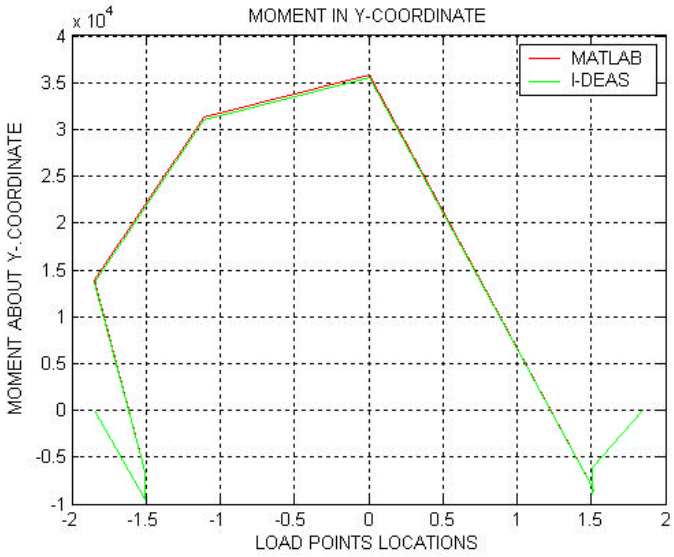

PlotD.2 Moment in Y-axis comparison.

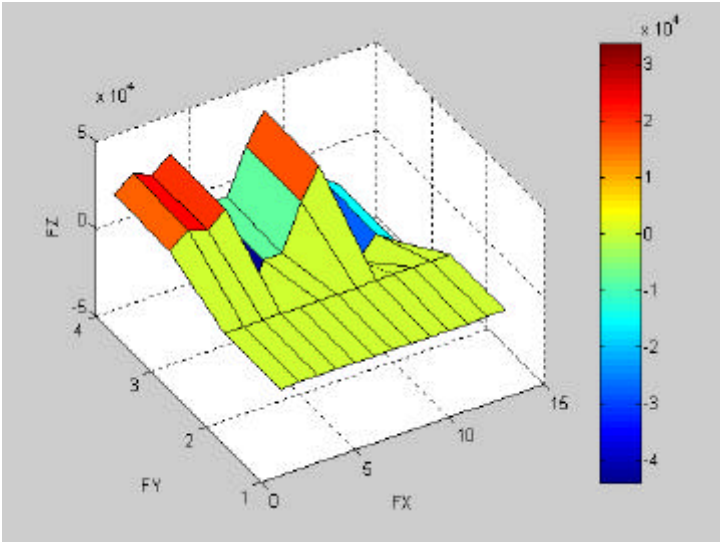

PlotD.3 Forces distribution in3D.

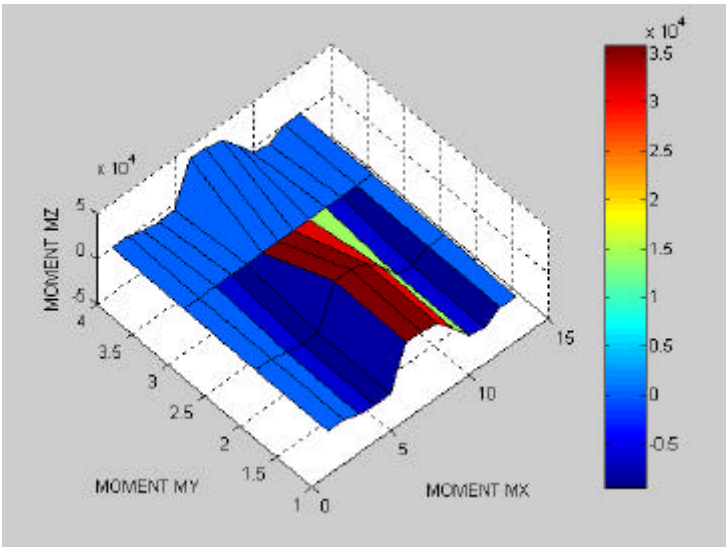

PlotD.4 Moment's distribution.

Appendix E

This appendix show the forces and moments value and their distributions of the pulling case

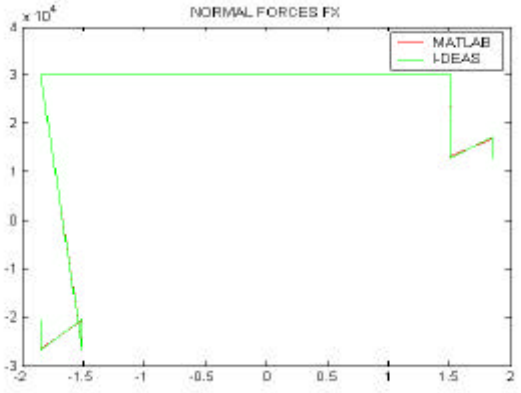

PlotE.1 Longitudinal force comparison.

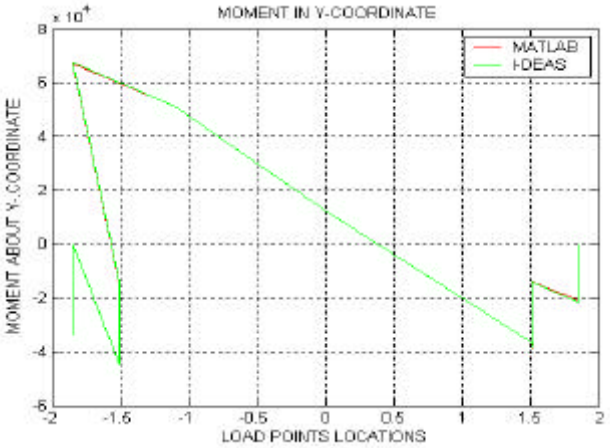

PlotE.2 Moment about y-axis comparison

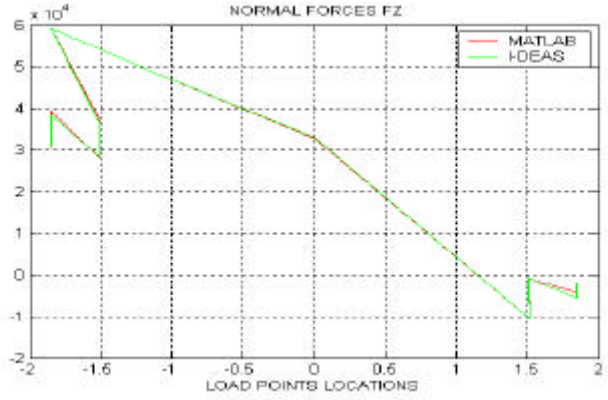

PlotE.3Normal force comparison

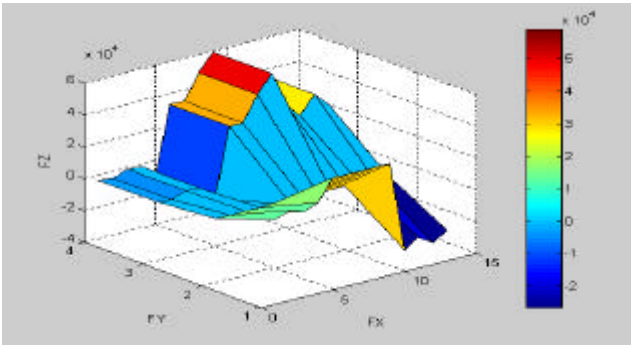

PlotE.4 Forces distribution

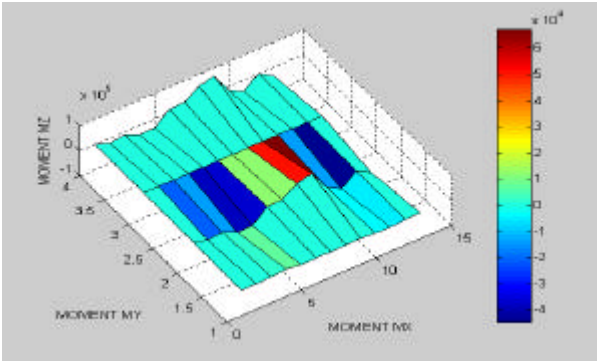

PlotE.5 Moments distribution

Appendix F

This appendix show the forces and moments value and their distributions of the towing case

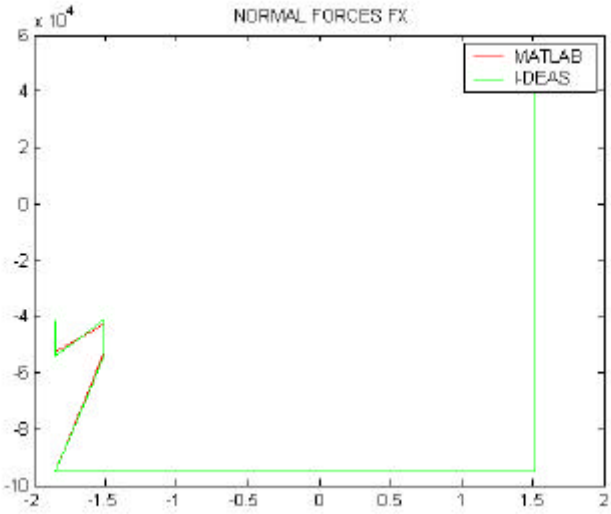

PlotF.1 Longitudinal comparison.

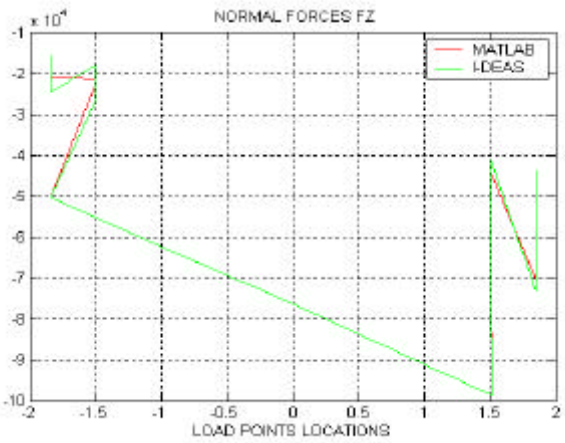

PlotF.2 Normal force comparison.

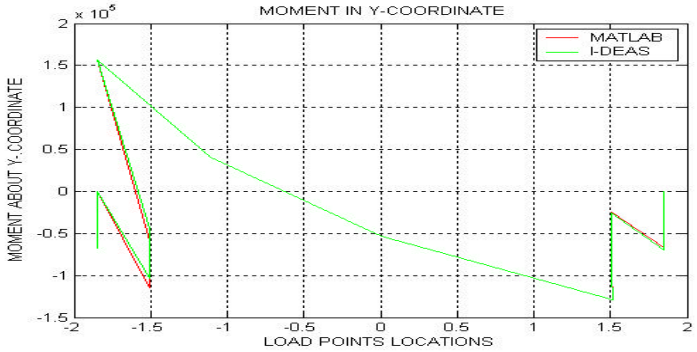

PlotF.3 Moment in Y-axis comparison.

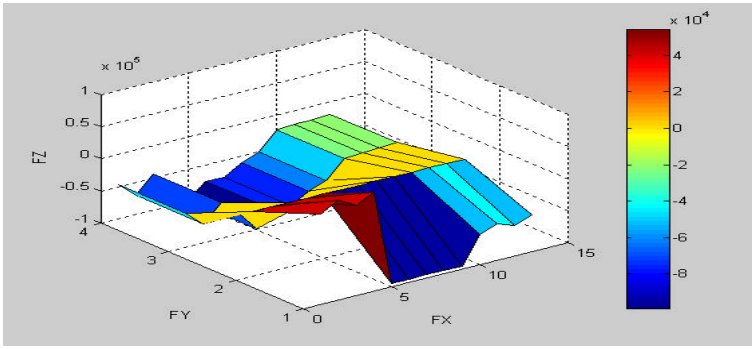

PlotF.4 Force distribution.

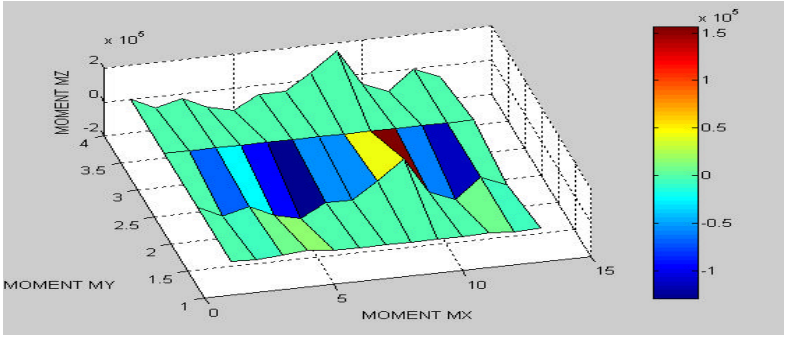

PlotF.5 Moment's distribution.

Appendix G

This appendix figures out the distribution of the forces and moments as well as the comparison between two models

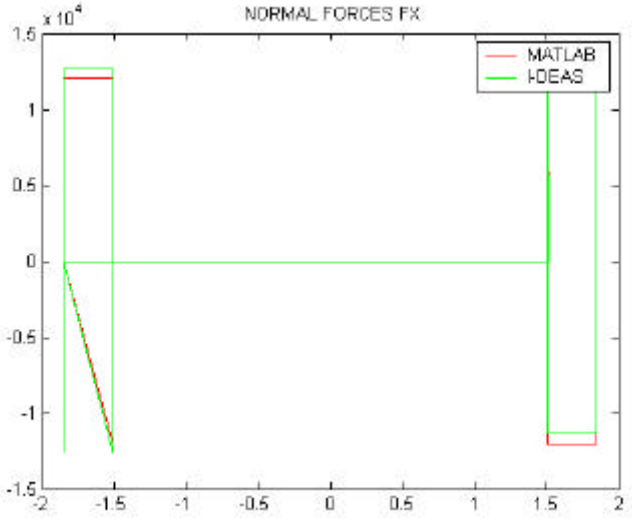

PlotG.1. Axial force comparison.

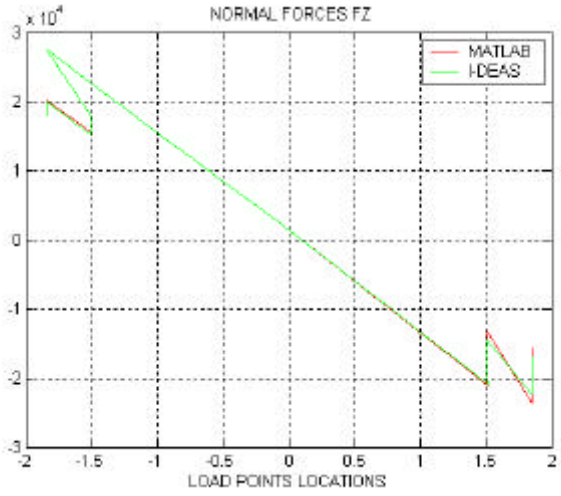

PlotG.2. Normal force comparison.

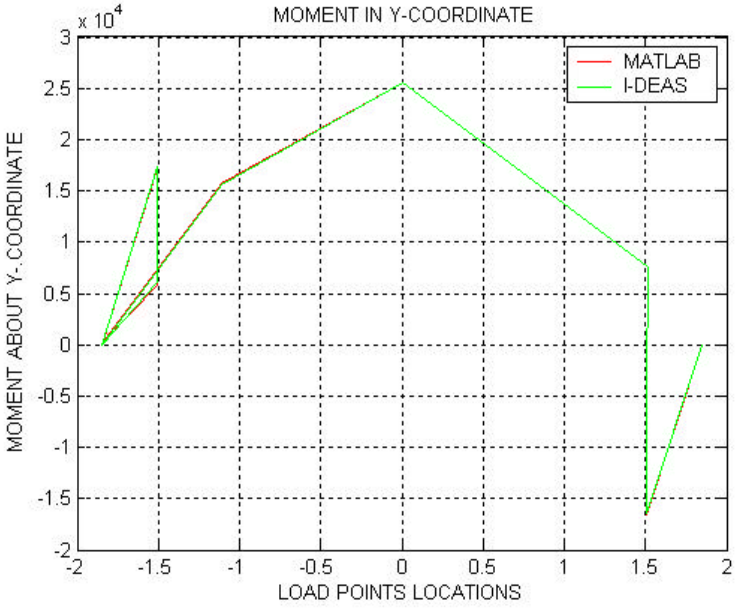

PlotG.3. Moment Y-axis comparison.

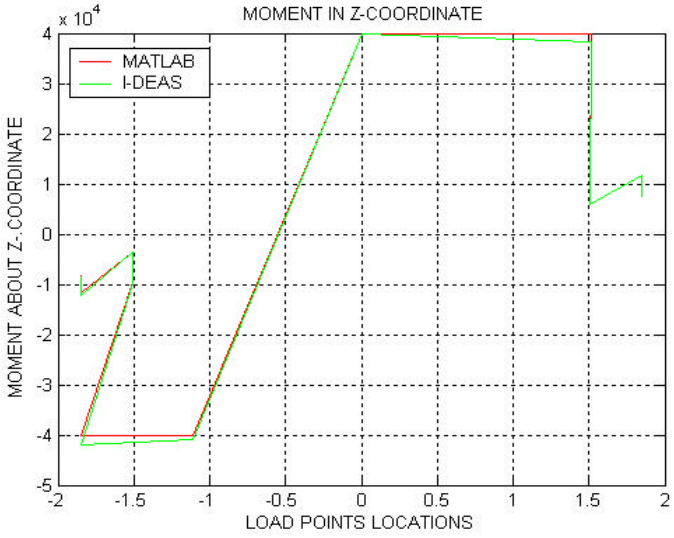

PlotG.4.Moment Z-axis comparison

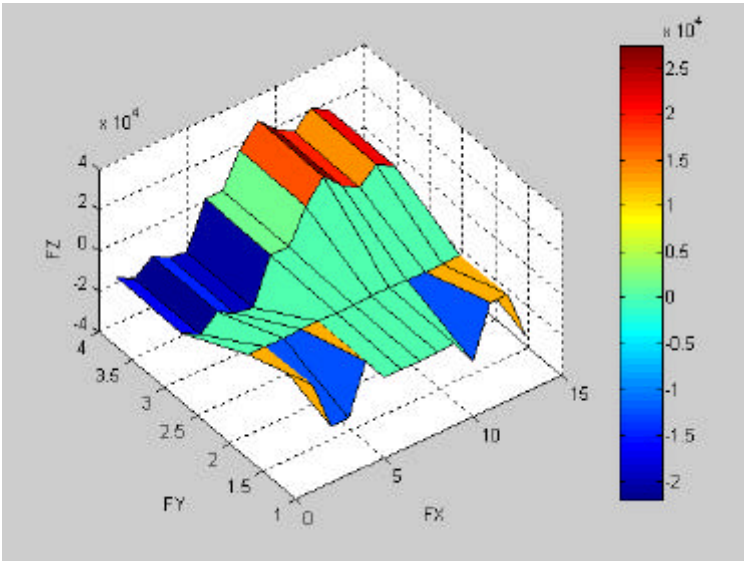

PlotG.5. Forces distribution.

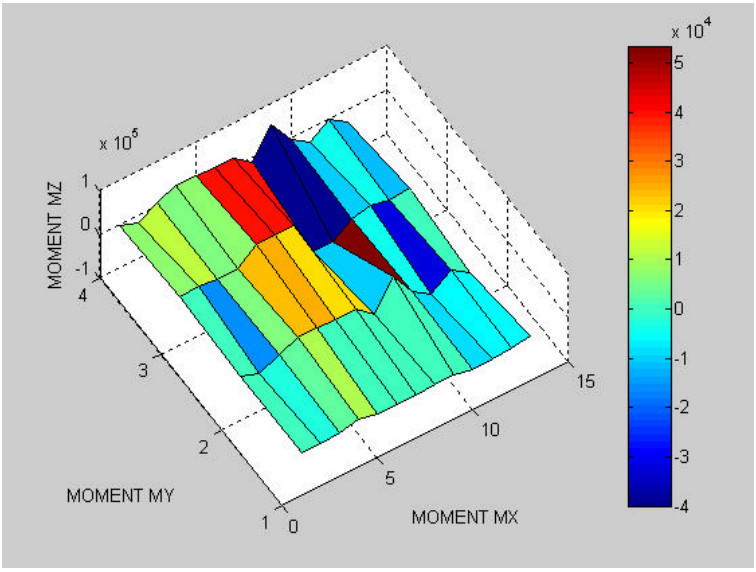

Plot G.6.Moments distribution.

Appendix H

This appendix shows the distribution of the forces and moments under lateral acceleration steering case

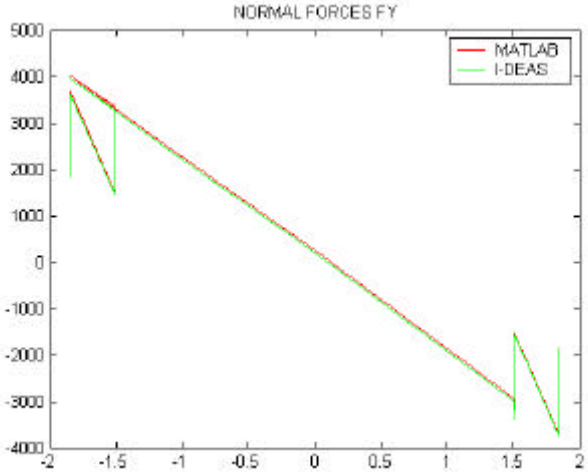

PlotE.1 Lateral forces comparison.

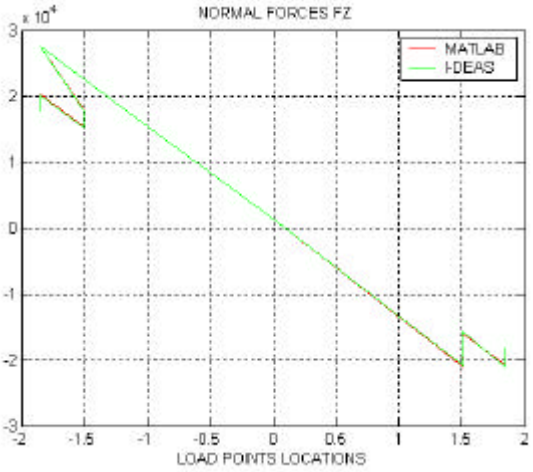

PlotE.2 Normal forces comparison.

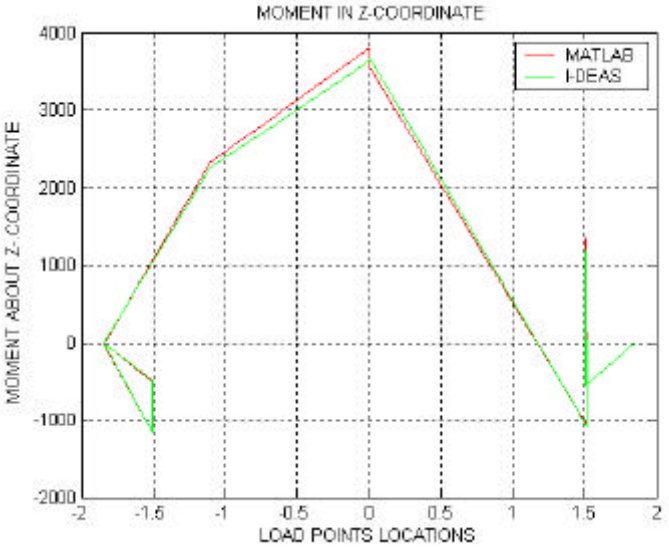

PlotE.3 Moment Z-axis comparison.

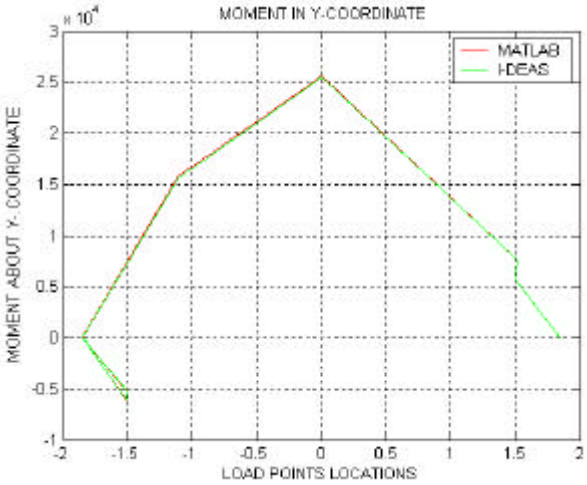

PlotE.4. Moment Y-axis comparison.

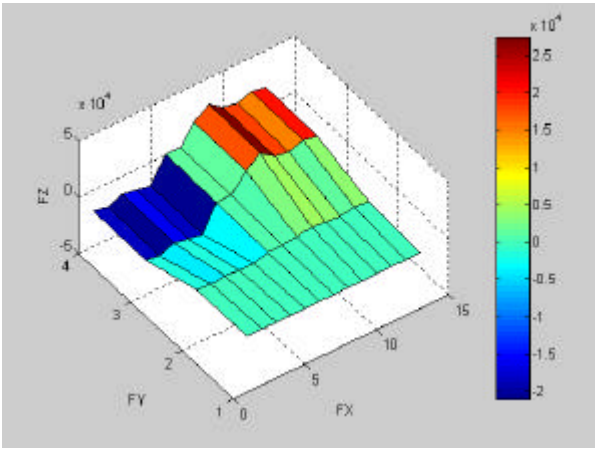

PlotE.5 Forces distribution.

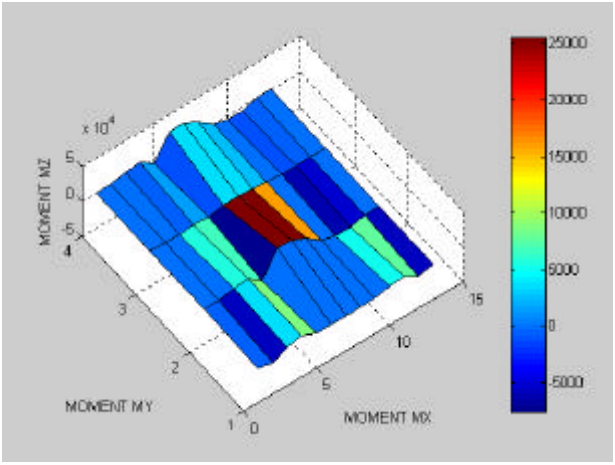

PlotE.6 Moments distribution.

Appendix I

This appendix shows some of the MAT LAB codes and functions that used to govern all equations according to the load case

Main script Roller_Force

inputloads

```
NLcase=10;  % NUMBER OF CASES


FX_1=zeros(NLcase);FZ_1=zeros(NLcase);FY_1=zeros(NLcase);MX_1=zeros(NLcase);MZ_1=zeros(NLcase);MY_1=zeros(NLcase);%EXTERNAL FORCES AND MOMENTS AT FRONT DRUM(VIB.SIDE)

FX_2=zeros(NLcase);FZ_2=zeros(NLcase);FY_2=zeros(NLcase);MX_2=zeros(NLcase);MZ_2=zeros(NLcase);MY_2=zeros(NLcase);%EXTERNAL FORCES AND MOMENTS AT THE FRONT DRUM(DRV.SIDE)

FX_3=zeros(NLcase);FZ_3=zeros(NLcase);FY_3=zeros(NLcase);MX_3=zeros(NLcase);MZ_3=zeros(NLcase);MY_3=zeros(NLcase);%EXTERNAL FORCES AND MOMENTS AT VIB.FORK EYELET

FX_4=zeros(NLcase);FZ_4=zeros(NLcase);FY_4=zeros(NLcase);MX_4=zeros(NLcase);MZ_4=zeros(NLcase);MY_4=zeros(NLcase);%EXTERNAL FORCES AT DRV.FORK EYELET

FX_5=zeros(NLcase);FZ_5=zeros(NLcase);FY_5=zeros(NLcase);MX_5=zeros(NLcase);MZ_5=zeros(NLcase);MY_5=zeros(NLcase);%EXTERNAL FORCES AND MOMENTS AT TOWING EYELET

FX_6=zeros(NLcase);FZ_6=zeros(NLcase);FY_6=zeros(NLcase);MX_6=zeros(NLcase);MZ_6=zeros(NLcase);MY_6=zeros(NLcase);%EXTERNAL FORCES AND MOMENTS AT REAR VIB.FORK EYELET

FX_7=zeros(NLcase);FZ_7=zeros(NLcase);FY_7=zeros(NLcase);MX_7=zeros(NLcase);MZ_7=zeros(NLcase);MY_7=zeros(NLcase);%EXTERNAL FORCES AND MOMENTS AT REAR DRV.FORK EYELET

FX_8=zeros(NLcase);FZ_8=zeros(NLcase);FY_8=zeros(NLcase);MX_8=zeros(NLcase);MZ_8=zeros(NLcase);MY_8=zeros(NLcase);%EXTERNAL FORCES AND MOMENTS AND MOMENTS AT PULLING EYELET

FX_9=zeros(NLcase);FZ_9=zeros(NLcase);FY_9=zeros(NLcase);MX_9=zeros(NLcase);MZ_9=zeros(NLcase);MY_9=zeros(NLcase);%EXTERNAL FORCES AND MOMENTS AT REAR DRUM(VIB.SIDE)

FX_10=zeros(NLcase);FZ_10=zeros(NLcase);FY_10=zeros(NLcase);MX_10=zeros(NLcase);MZ_10=zeros(NLcase);MY_10=zeros(NLcase;%EXTERNAL FORCES AND MOMENTS AT THE REAR DRUM(DRV.SIDE)
```

```
NLcase=10;  % NUMBER OF CASES

Fx_1=zeros(NLcase);Fz_1=zeros(NLcase);Fy_1=zeros(NLcase);Mx_1=zeros(NLcase
);My_1=zeros(NLcase);Mz_1=zeros(NLcase);%INTERNAL ELEMENT FORCES
AND MOMENTS AT FRONT DRUM(VIB.SIDE)

Fx_2=zeros(NLcase);Fz_2=zeros(NLcase);
Fy_2=zeros(NLcase);Mx_2=zeros(NLcase);My_2=zeros(NLcase);Mz_2=zeros(NLca
se);%INTERNAL ELEMENT FORCES AND MOMENTS AT FRONT
DRUM(VIB.SIDE)

Fx_3=zeros(NLcase);Fz_3=zeros(NLcase);Fy_3=zeros(NLcase);Mx_3=zeros(NLcase
);My_3=zeros(NLcase);Mz_3=zeros(NLcase);%INTERNAL ELEMENT FORCES
AND MOMENTS AT VIB.FORK

Fx_4=zeros(NLcase);Fz_4=zeros(NLcase);Fy_4=zeros(NLcase);Mx_4=zeros(NLcase
);My_4=zeros(NLcase);Mz_4=zeros(NLcase);%INTERNAL ELEMENT FORCES
AND MOMENTS  AT DRV.FORK

Fx_5=zeros(NLcase);Fz_5=zeros(NLcase);Fy_5=zeros(NLcase);Mx_5=zeros(NLcase
);My_5=zeros(NLcase);Mz_5=zeros(NLcase);%INTERNAL ELEMENT FORCES
AND MOMENTS OF THE MASS MS

Fx_6=zeros(NLcase);Fz_6=zeros(NLcase);Fy_6=zeros(NLcase);Mx_6=zeros(NLcase
);My_6=zeros(NLcase);Mz_6=zeros(NLcase);%INTERNAL ELEMENT FORCES
AND MOMENTS AT THE FRONT STEERING HITCH

Fx_7=zeros(NLcase);Fz_7=zeros(NLcase);Fy_7=zeros(NLcase);Mx_7=zeros(NLcase
);My_7=zeros(NLcase);Mz_7=zeros(NLcase);%INTERNA ELEMENT FORCES
AND MOMENTS AT THE REAR STEERING HITCH

Fx_8=zeros(NLcase);Fz_8=zeros(NLcase);Fy_8=zeros(NLcase);Mx_8=zeros(NLcase
);My_8=zeros(NLcase);Mz_8=zeros(NLcase);%INTERNAL ELEMENT FORCES
AND MOMENTS OF THE MASS MK

Fx_9=zeros(NLcase);Fz_9=zeros(NLcase);Fy_9=zeros(NLcase);Mx_9=zeros(NLcase
);My_9=zeros(NLcase);Mz_9=zeros(NLcase);%INTERNAL ELEMENT FORCES
AND MOMENTS OF THE MASS MH

Fx_10=zeros(NLcase);Fz_10=zeros(NLcase);Fy_10=zeros(NLcase);Mx_10=zeros(N
Lcase);My_10=zeros(NLcase);Mz_10=zeros(NLcase);%INTERNAL ELEMENT
AND MOMENTS FORCES AT REAR VIB.FORK

Fx_11=zeros(NLcase);Fz_11=zeros(NLcase);Fy_11=zeros(NLcase);Mx_11=zeros(N
Lcase);My_11=zeros(NLcase);Mz_11=zeros(NLcase);%INTERNAL ELEMENT
AND MOMENTS FORCES AT REAR DRV.FORK

Fx_12=zeros(NLcase);Fz_12=zeros(NLcase);Fy_12=zeros(NLcase);Mx_12=zeros(N
Lcase);My_12=zeros(NLcase);Mz_12=zeros(NLcase);%INTERNAL ELEMENT
AND MOMENTS FORCES AT REAR DRUM(VIB.SIDE)
```

```
Fx_13=zeros(NLcase);Fz_13=zeros(NLcase);Fy_13=zeros(NLcase);Mx_13=zeros(NLcase);My_13=zeros(NLcase);Mz_13=zeros(NLcase);%INTERNAL ELEMENT FORCES AND MOMENTS AT REAR DRUM(VIB.SIDE)

%%%%%%%%%%%%%%%%%%%%%%%%%%%%%%%%%%%%%%%%%%%%%%%%%%%%%%%%%%%%%%%%%%%%%%%%%%

% GRAVITY MODEL

%%%%%%%%%%%%%%%%%%%%%%%%%%%%%%%%%%%%%%%%%%%%%%%%%%%%%%%%%%%%%%%%%%%%%%%%%%

%EXTERNAL LOADS MATRIX

%%%%%%%%%%%%%%%%%%%%%%%%%%%%%%%%%%%%%%%%%%%%%%%%%%%%%%%%%%%%%%%%%%%%%%%%%%

LC=1;

acc=[0 0 g]; %ACCELERATION VECTOR

XDIM1=[x2 0 0 0;1 1 0 0]; % DIMENTION MATRIX

MY1=[mt*acc(3)*(xt+x3)*cos(teta)-mt*acc(3)*(zt+z2)*sin(teta);mt*acc(3)*cos(teta)];% MATRIX INCLUDES THE SUM OF FORCES AND MOMENTS IN Z AND Y-AXIS

GRAVMTORQUE(LC,0,XDIM1,MY1,acc,1,1);% FUNCTION THAT COMBINE GRAVITY AND MAXIMUM TORQUE CASE


%%%%%%%%%%%%%%%%%%%%%%%%%%%%%%%%%%%%%%%%%%%%%%%%%%%%%%%%%%%%%%%%%%%%%%%%%%

% ACCELERATION MODEL

%%%%%%%%%%%%%%%%%%%%%%%%%%%%%%%%%%%%%%%%%%%%%%%%%%%%%%%%%%%%%%%%%%%%%%%%%%

%EXTERNAL LOADS MATRIX

%%%%%%%%%%%%%%%%%%%%%%%%%%%%%%%%%%%%%%%%%%%%%%%%%%%%%%%%%%%%%%%%%%%%%%%%%%

LC=2;

acc1=[0.5*g  0  g];%ACCELERATION VECTOR

XDIM2=[x2 0 0 0;1 1 0 0;-etaf 0 1 0;0 -etar 0 1];%MATRIX INCLUDES THE DIMENTION AND COEFFICIENT OF FRICTION

MY2=[mt*acc1(3)*(x3+xt)*cos(teta)-mt*acc1(3)*sin(teta)*(zt+z2)-acc1(1)*mt*(zt+z2);mt*g*cos(teta);0;0];% MATRIX INCLUDES THE SUM OF FORCES AND MOMENTS IN Z AND Y-AXIS

ACCELERATION(LC,XDIM2,MY2,acc1,1,1,1,1);% FUNCTION THAT IMPLEMENT THE ACCELERATION CASE

%%%%%%%%%%%%%%%%%%%%%%%%%%%%%%%%%%%%%%%%%%%%%%%%%%%%%%%%%%%%%%%%%%%%%%%%

% LIFTING MODEL

%%%%%%%%%%%%%%%%%%%%%%%%%%%%%%%%%%%%%%%%%%%%%%%%%%%%%%%%%%%%%%%%%%%%%%%%

%EXTERNAL TENSION LOADS MATRIX
```

```
%%%%%%%%%%%%%%%%%%%%%%%%%%%%%
LC=3;
acc2=[0 0 1.6*g]; %ACCELERATION VECTOR
MY3=[2*x6 -2*x7;2 2];
FORCE3=[0; mt*acc2(3)];
LIFTING(LC,MY3,FORCE3,acc2,2,2);
%%%%%%%%%%%%%%%%%%%%%%%%%%%%%%%%%%%%%
% PULLING MODEL
%%%%%%%%%%%%%%%%%%%%%%%%%%%%%%%%%%%%%
%EXTERNAL LOADS MATRIX
%%%%%%%%%%%%%%%%%%%%%%%%%%%%%%%%%%%%%
LC=4;
acc3=[0 0 g]; %ACCELERATION VECTOR
XDIM4=[x2 0 0 0;
   1 1 0 0;
   0 0 1 1;
   0 -etar 0 1];
MY4=[mt*g*(x3+xt)*cos(teta)-Fpull*(z5+z2)-mt*g*sin(teta)*(zt+z2);
   mt*g*cos(teta);
   Fpull+mt*g*sin(teta);
   0];

PULLING(LC,XDIM4,MY4,acc3,1,1,1,1);
%%%%%%%%%%%%%%%%%%%%%%%%%%%%%%%%%%%%%
% TOWING MODEL
%%%%%%%%%%%%%%%%%%%%%%%%%%%%%%%%%%%%%
%EXTERNAL LOADS MATRIX
%%%%%%%%%%%%%%%%%%%%%%%%%%%%%%%%%%%%%
LC=5;
XDIM5=[x1+x3 0 0 ;
     1 1 0 ;
     0 0 1 ];
```

```
MY5=[mt*g*(xt+x3)*cos(teta)+1.5*g*mt*(z5+z2);
   mt*g*cos(teta);
   1.5*g*mt-mt*g*sin(teta)];

TOWING(LC,XDIM5,MY5,acc,2,2,2,2);
%%%%%%%%%%%%%%%%%%%%%%%%%%%%%%%%%%%%%%%%%%%%%%%%%%%%%%%%
% MAXIMUM TORQUE UNDER GRAVITY SET
%%%%%%%%%%%%%%%%%%%%%%%%%%%%%%%%%%%%%%%%%%%%%%%%%%%%%%%%
% EXTERNAL LOAD MATRIX AND INPUT TORQUE
%%%%%%%%%%%%%%%%%%%%%%%%%%%%%%%%%%%%%%%%%%%%%%%%%%%%%%%%
LC=6;
XDIM1=[x2 0 0 0;1 1 0 0;0 0 r 0;0 0 0 r];
MY1=[mt*acc(3)*(xt+x3)*cos(teta)-mt*acc(3)*(zt+z2)*sin(teta)-
2*Tbrake;mt*acc(3)*cos(teta);Tbrake;Tbrake];
GRAVMTORQUE(LC,Tbrake,XDIM1,MY1,acc,1,1);
%%%%%%%%%%%%%%%%%%%%%%%%%%%%%%%%%%%%%%%%%%%%%%%%%%%%%%%%
% STEERING LOADS UNDER GRAVITY AND LATERAL ACCELERATION
MODEL
%%%%%%%%%%%%%%%%%%%%%%%%%%%%%%%%%%%%%%%%%%%%%%%%%%%%%%%%
% EXTERNAL LOAD MATRIX
%%%%%%%%%%%%%%%%%%%%%%%%%%%%%%%%%%%%%%%%%%%%%%%%%%%%%%%%
%steering load case (lateral acceleration  load case)
LC=7;
ay=velocity^2/R;%LATERAL ACCELERATION
acc4=[0 ay g];%ACCELERATION VECTOR
XDIM8=[x2 0 ;1 1 ];% DIMENSION MATRIX
MY8=[mt*acc(3)*(xt+x3)*cos(teta)-mt*acc(3)*(zt+z2)*sin(teta);mt*acc(3)*cos(teta)];%
MATRIX INCLUDES THE SUM OF FORCES AND MOMENTS IN Z AND Y-AXIS
LATERALACC(LC,ay,acc4,XDIM8,MY8,2,2); %FUNCTION THAT CACULATES THE
FORCES AND MOMENTS OF LATERAL CASE
%%%%%%%%%%%%%%%%%%%%%%%%%%%%%%%%%%%%%%%%%%%%%%%%%%%%%%%%
% STEERING LOADS UNDER GRAVITY ACCELERATION MODEL A
%%%%%%%%%%%%%%%%%%%%%%%%%%%%%%%%%%%%%%%%%%%%%%%%%%%%%%%%
% EXTERNAL LOAD MATRIX WITH DISTRIBUTED LOAD CONSIDRED
```

%%%

LC=8;

acc=[0 0 g];%ACCELERATION VECTOR

XDIM9=[x2 0;1 1];% DIMENSION MATRIX

MY9=[mt*acc(3)*(xt+x3);mt*acc(3)];% MATRIX INCLUDES THE SUM OF FORCES AND MOMENTS IN Z AND Y-AXIS

STEERMODELA(LC,XDIM9,MY9,acc,2,2,2,2); %FUNCTION THAT CACULATES THE FORCES AND MOMENTS OF STEERING UNDER GRAVITY

%%%

% STEERING LOADS UNDER GRAVITY ACCELERATION MODEL B

%%%

% EXTERNAL LOAD MATRIX

%%%

LC=9;

XDIM10=[x2 0;1 1];% DIMENSION MATRIX

MY10=[mt*acc(3)*(xt+x3);mt*acc(3)];% MATRIX INCLUDES THE SUM OF FORCES AND MOMENTS IN Z AND Y-AXIS

STEERMODELB(LC,XDIM10,MY10,acc,2,2,2,2);%FUNCTION THAT CACULATES THE FORCES AND MOMENTS OF STEERING UNDER GRAVITY

%%%

% STEERING LOADS UNDER GRAVITY ACCELERATION MODEL C

%%%

% EXTERNAL LOAD MATRIX

%%%

LC=10;

XDIM11=[x2 0;1 1];% DIMENSION MATRIX

MY11=[mt*acc(3)*(xt+x3);mt*acc(3)];% MATRIX INCLUDES THE SUM OF FORCES AND MOMENTS IN Z AND Y-AXIS

STEERMODELC(LC,XDIM11,MY11,acc,2,2,2,2);%FUNCTION THAT CACULATES THE FORCES AND MOMENTS OF STEERING UNDER GRAVITY

Outtext

Department of Mechanical Engineering, Master's Degree Programme
Blekinge Institute of Technology, Campus Gräsvik
SE-371 79 Karlskrona, SWEDEN

Telephone: +46 455-38 55 10
Fax: +46 455-38 55 07
E-mail: ansel.berghuvud@bth.se